Journal of Visualized Experiments

Applications of spatio-temporal mapping and particle analysis techniques to quantify intracellular Ca2+ signaling in situ

--Manuscript Draft--

Article Type:	Methods Article - JoVE Produced Video
Manuscript Number:	JoVE58989R1
Full Title:	Applications of spatio-temporal mapping and particle analysis techniques to quantify intracellular Ca2+ signaling in situ
Keywords:	Ca2+ imaging ImageJ Interstitial cell of Cajal Confocal Microscopy Ano1 gastrointestinal motility small intestine GCaMP Ca2+ wave Ca2+ release spatio-temporal map particle analysis
Corresponding Author:	Bernard T Drumm, Ph.D University of Nevada, Reno School of Medicine Reno, Nevada UNITED STATES
Corresponding Author's Institution:	University of Nevada, Reno School of Medicine
Corresponding Author E-Mail:	bdrumm@med.unr.edu
Order of Authors:	Bernard T Drumm, Ph.D
	Grant W. Hennig
	Salah A. Baker
	Kenton M. Sanders
Additional Information:	
Question	**Response**
Please indicate whether this article will be Standard Access or Open Access.	Standard Access (US$2,400)
Please indicate the **city, state/province, and country** where this article will be **filmed**. Please do not use abbreviations.	Reno, NV, U.S.A.

Cover Letter

Bernard T. Drumm, Ph.D
Research Assistant Professor
Dept. Physiology & Cell Biology
Anderson Health Sciences

University of Nevada, Reno
School of Medicine

October 3rd 2018

Dear Editor,

Please find attached in the submission materials our revised manuscript entitled "**Applications of spatio-temporal mapping and particle analysis techniques to quantify intracellular Ca^{2+} signaling *in situ*"** by Bernard T. Drumm, Grant W. Hennig, Salah A. Baker and Kenton M. Sanders for consideration for publication in JoVE. Our manuscript describes detailed protocols used in our laboratory to quantify Ca^{2+} imaging recordings acquired from *in situ* intact tissue preparations.

As outlined in our original submission, the protocols described in our paper facilitate a more complete analysis and quantification of Ca^{2+} signals recorded from cells *in situ* using a combination of spatiotemporal map (STM)-based analysis and particle-based analysis. For illustration, the protocols will examine Ca^{2+} signalling in a specialized population of cells in the small intestine, interstitial cells of Cajal (ICC). These protocols can also be applied to other cell types within other preparations and thus should provide a valuable tool for other researchers that wish to more completely describe Ca^{2+} dynamics in their experiments.

We would like to thank the reviewing editor and referees for the careful consideration and examination of our work. After the decision letter received on 09/21/2018 we have completed the revisions requested by the reviewing editor and all 4 reviewers. Our revised manuscript and figures are attached and our point-by-point responses to the editorial and reviewers comments (shown in blue in the document) are also attached.

Thank you for the consideration of our revised manuscript.

Bernard T Drumm, PhD

Bernard T. Drumm, Ph.D • 1664 N. Virginia Street • Reno, NV 89557 • (775) 685-0975 • bdrumm@med.unr.edu

Title:

Applications of Spatio-temporal Mapping and Particle Analysis Techniques to Quantify Intracellular Ca^{2+} Signaling *In situ*

Authors and Affiliations:

Bernard T. Drumm[1], Grant W. Hennig[2], Salah A. Baker[1] & Kenton M. Sanders[1].

[1]Department of Physiology and Cell Biology, University of Nevada Reno School of Medicine, Reno, NV 89557, USA

[2]Department of Pharmacology, The Robert Larner, M.D. College of Medicine, University of Vermont, Burlington, VT, United States

Corresponding author:

Bernard T. Drumm (bdrumm@med.unr.edu)

Tel: (775) 685-0975

Email Addresses of Co-authors:

Grant W. Hennig (grant.hennig@med.uvm.edu)

Salah A. Baker (sabubaker@med.unr.edu)

Kenton M. Sanders (ksanders@med.unr.edu)

Keywords:

Ca^{2+} imaging, ImageJ, interstitial cell of Cajal, confocal microscopy, Ano1, gastrointestinal motility, small intestine, GCaMP, Ca^{2+} wave, Ca^{2+} release, spatio-temporal map, particle analysis

Short abstract:

Genetically encoded Ca^{2+} indicators (GECIs) have radically changed how *in situ* Ca^{2+} imaging is performed. To maximize data recovery from such recordings, appropriate analysis of Ca^{2+} signals is required. The protocols in this paper facilitate the quantification of Ca^{2+} signals recorded *in situ* using spatiotemporal mapping and particle-based analysis.

Long abstract:

Ca^{2+} imaging of isolated cells or specific types of cells within intact tissues often reveals complex patterns of Ca^{2+} signaling. This activity requires careful and in-depth analyses and quantification to capture as much information about the underlying events as possible. Spatial, temporal and intensity parameters intrinsic to Ca^{2+} signals such as frequency, duration, propagation, velocity and amplitude may provide some biological information required for intracellular signalling. High-resolution Ca^{2+} imaging typically results in the acquisition of large data files that are time consuming to process in terms of translating the imaging information into quantifiable data, and this process can be susceptible to human error and bias. Analysis of Ca^{2+} signals from cells *in situ* typically relies on simple intensity measurements from arbitrarily selected regions of interest (ROI) within a field of view (FOV). This approach ignores much of the important signaling information contained in the FOV. Thus, in order to maximize recovery of information from such high-resolution recordings obtained with Ca^{2+}dyes or optogenetic Ca^{2+} imaging, appropriate

spatial and temporal analysis of the Ca^{2+} signals is required. The protocols outlined in this paper will describe how a high volume of data can be obtained from Ca^{2+} imaging recordings to facilitate more complete analysis and quantification of Ca^{2+} signals recorded from cells using a combination of spatiotemporal map (STM)-based analysis and particle-based analysis. The protocols also describe how different patterns of Ca^{2+} signaling observed in different cell populations *in situ* can be analyzed appropriately. For illustration, the method will examine Ca^{2+} signaling in a specialized population of cells in the small intestine, interstitial cells of Cajal (ICC), using GECIs.

Introduction:

Ca^{2+} is a ubiquitous intracellular messenger which controls a wide range of cellular processes, such as muscle contraction[1,2], metabolism[3], cell proliferation[3–5], stimulation of neurotransmitter release at nerve terminals[6,7], and activation of transcription factors in the nucleus.[7] Intracellular Ca^{2+} signals often take the form of transient elevations in cytosolic Ca^{2+}, and these can be spontaneous or arise from agonist stimulation depending on the cell type[8]. Spatial, temporal and intensity parameters intrinsic to Ca^{2+} signals such as frequency, duration, propagation, velocity, and amplitude can provide the biological information required for intracellular signalling[5,7,9]. Cytoplasmic Ca^{2+} signals can result from the influx of Ca^{2+} from the extracellular space or via Ca^{2+} release from the endoplasmic reticulum (ER) via Ca^{2+} release channels such as ryanodine receptors (RyRs) and inositol-tri-phosphate receptors (IP_3Rs)[10]. RyRs and IP_3Rs may both contribute to the generation of Ca^{2+} signals and the concerted opening of these channels, which combined with various Ca^{2+} influx mechanisms can result in a myriad of Ca^{2+} signalling patterns that are shaped by the numbers and open probability of Ca^{2+} influx channels, the expression profile of Ca^{2+} release channels, the proximity between Ca^{2+} influx and release channels, and expression and distribution of Ca^{2+} reuptake and extrusion proteins. Ca^{2+} signals may take the form of uniform, long lasting, high intensity global oscillations that may last for several seconds or even minutes, propagating intracellular and intercellular Ca^{2+} waves that may cross intracellular distances over 100 µm[10–16], or more brief, spatially localized events such as Ca^{2+} sparks and Ca^{2+} puffs that occur on tens of millisecond timescales and spread less than 5 µm[17–20].

Fluorescent microscopy has been used widely to monitor Ca^{2+} signalling in isolated and cultured cells and in intact tissues. Traditionally, these experiments involved the use of fluorescent Ca^{2+} indicators, ratiometric and non-ratiometric dyes such as Fura2, Fluo3/4 or Rhod2, among others [21–23]. These indicators were designed to be permeable to cell membranes and then become trapped in cells by the cleavage of an ester group via endogenous esterases. Binding of Ca^{2+} to the high affinity indicators caused changes in fluorescence when the cells and tissues were illuminated by appropriate wavelengths of light. The use of cell permeable Ca^{2+} indicators greatly enhanced our understanding of Ca^{2+} signaling in living cells and permitted spatial resolution and quantification of these signals that was not possible by assaying Ca^{2+} signals through other means, such as electrophysiology. However, traditional Ca^{2+} indicators have several limitations, such as photobleaching that occurs over extended recording periods[24]. While newer Ca^{2+} indicator dyes such as Cal520/590 have greatly improved signal to noise ratios and the ability to

detect local Ca^{2+} signals[25], issues with photobleaching can still remain a concern for some investigators[26–28]. Precipitous photobleaching also restricts the magnification, rate of image acquisition, and resolution that can be used for recordings, as increased objective power and higher rates of image acquisition require increased excitation light intensity that increases photobleaching.

These limitations of traditional Ca^{2+} indicator dyes are exacerbated when recording Ca^{2+} signals *in situ*, for example when recording intracellular Ca^{2+} signals from intact tissues. Due to the problems above, visualization of Ca^{2+} signals *in situ* using cell permeable Ca^{2+} indicators has been limited to low power magnification and reduced rates of image capture, constraining the ability of investigators to record and quantify temporally or spatially restricted subcellular Ca^{2+} signals. Thus, it has been difficult to capture, analyze, and appreciate the spatial and temporal complexity of Ca^{2+} signals, which can be important in the generation of desired biological responses, as outlined above. Analysis of Ca^{2+} signals from cells *in situ* typically relies on simple intensity measurements from selected regions of interest (ROI) within a field of view (FOV). The arbitrary choice of the number, size and position of ROIs, dependent on the whim of the researcher, can severely bias the results obtained. As well as inherent bias with ROI analysis, this approach ignores much of the important signaling information contained in the FOV, as dynamic Ca^{2+} events within an arbitrarily chosen ROI are selected for analysis. Furthermore, analysis of ROIs fails to provide information about the spatial characteristics of the Ca^{2+} signals observed. For example, it may not be possible to distinguish between a rise in Ca^{2+} resulting from a propagating Ca^{2+} wave and a highly localized Ca^{2+} release event from tabulations of Ca^{2+} signals within an ROI.

The advent of genetically encoded Ca^{2+} indicators (GECIs) has radically changed how Ca^{2+} imaging can be performed *in situ*[29–33]. There are several advantages to using GECIs over dyes. The most important perhaps is that expression of GECI can be performed in a cell specific manner, which reduces unwanted background contamination from cells not of interest. Another advantage of GECIs over traditional Ca^{2+} indicators is that photobleaching is reduced (as fluorescence and consequentially photobleaching only occurs when cells are active), as compared to dye-loaded specimens, particularly at high magnification and high rates of image capture[34]. Thus, imaging with GECIs, such as the GCaMP series of optogenetic sensors, affords investigators the ability to record brief, localized sub-cellular Ca^{2+} signals *in situ* and investigate Ca^{2+} signaling in cells within their native environments that have not been possible previously. To maximize recovery of information from such high-resolution recordings, appropriate spatial and temporal analysis of the Ca^{2+} signals is required. It should be noted that while GECIs can offer some clear advantages, recent studies have revealed that Ca^{2+} imaging can be successfully performed from large populations of different neurochemical classes of neurons simultaneously using conventional Ca^{2+} indicators that are not genetically encoded into the animal[35]. This approach used *post hoc* immunohistochemistry to reveal multiple different classes of neurons firing at high frequency in synchronized bursts, and avoided the potential that genetic modifications to the animal may have interfered with the physiological behavior the investigator seeks to understand[35,36].

The protocols outlined in this paper facilitate more complete analysis and quantification of Ca^{2+} signals recorded from cells *in situ* using a combination of spatiotemporal map (STM)-based

analysis and particle-based analysis. The protocols also describe how different patterns of Ca^{2+} signaling observed in different cell populations *in situ* can be analyzed appropriately. For illustration, the method will examine Ca^{2+} signalling in a specialized population of cells in the small intestine, interstitial cells of Cajal (ICC). ICC are specialized cells in the gastrointestinal (GI) tract that exhibit dynamic intracellular Ca^{2+} signaling, as visualized using mice expressing GCaMPs[37–42]. Ca^{2+} transients in ICC are linked to activation of Ca^{2+}-activated Cl^- channels (encoded by *Ano1*) that are important in regulating the excitability of intestinal smooth muscle cells (SMCs)[43–45]. Thus, the study of Ca^{2+} signaling in ICC is fundamental to understanding intestinal motility. The murine small intestine offers an excellent example for this demonstration, as there are two classes of ICC that are anatomically separated and can be visualized independently: i) ICC are located in the area between the circular and longitudinal smooth muscle layers, surrounding the myenteric plexus (ICC-MY). These cells serve as pacemaker cells and generate the electrical activity known as slow waves[46–49]; ii) ICC are also located amongst a plexus rich in the terminals of motor neurons (deep muscular plexus, thus ICC-DMP). These cells serve as mediators of responses to enteric motor neurotransmission[37,39,40,50]. ICC-MY and ICC-DMP are morphologically distinct, and their Ca^{2+} signaling behaviors differ radically to accomplish their specific tasks. ICC-MY are stellate in shape and form a network of interconnected cells via gap junctions[51,52]. Ca^{2+} signals in ICC-MY manifest as brief and spatially localized Ca^{2+} release events occurring at multiple sites asynchronously through the ICC-MY network as visualized within a FOV (imaged with a 60X objective)[38]. These asynchronous signals are organized temporally into 1 second clusters that, when tabulated together, amount to a net 1 s cellular rise in Ca^{2+}. These signals propagate cell-to-cell within the ICC network and therefore organize Ca^{2+} signaling, generated from sub-cellular sites, into a tissue wide Ca^{2+} wave. Temporal clustering and summation of Ca^{2+} signals in ICC-MY has been termed Ca^{2+} transient clusters (CTCs)[38]. CTCs occur rhythmically (*e.g.* quite similar durations and similar periods between CTCs) 30 times per minute in the mouse. Conversely, ICC-DMP are spindle shaped cells, some with secondary processes, that distribute between SMCs and varicose nerve processes and do not independently form a network[51,52]. ICC-DMP form gap junctions with SMCs, however, and function within this greater syncytium, known as the SIP syncytium[53]. Ca^{2+} signals occur at multiple sites along the lengths of cells, but these transients are not entrained or temporally clustered, as observed in ICC-MY[37]. Ca^{2+} signals in ICC-DMP occur in a stochastic manner, with variable intensities, durations and spatial characteristics. The protocols below, using the example of Ca^{2+} signaling in ICC-MY and ICC-DMP, describe techniques to analyze complex signaling in specific types of cells *in situ*. We utilized the inducible Cre-Lox p system to express GCaMP6f exclusively in ICC, after inducing activation of Cre-Recombinase (Cre) driven by an ICC specific promoter (*Kit*).

Protocol:

All animals used and the protocols carried out in this study were in accordance with the National Institutes of Health Guide for the Care and Use of Laboratory Animals. All procedures were approved by the Institutional Animal Use and Care Committee at the University of Nevada, Reno.

1. Generation of KitGCaMP6f Mice

1.1. Cross Ai95 (RCL-GCaMP6f)-D (GCaMP6f mice) and c-Kit$^{+/Cre\text{-}ERT2}$ (Kit-Cre mice) to generate ICC specific GCaMP6f expressing animals (Kit-Cre-GCaMP6f mice).

NOTE: GCaMP6f was used due to its reported efficiency in reporting localized, brief intracellular Ca^{2+} signals *in situ* and *in vivo*[54].

1.2. Inject Kit-Cre-GCaMP6f mice with tamoxifen at ages of 6-8 weeks to induce Cre Recombinase activation and subsequent GCaMP6f expression in ICC (**Figure 1**).

1.2.1. To create the tamoxifen solution, dissolve 80 mg of Tamoxifen (see **Table of Materials**) in 800 µL of ethanol (see **Table of Materials**) in a cuvette and vortex for 20 minutes.

1.2.2. Add 3.2 mL of safflower oil (generic) to create solutions of 20 mg/mL and then sonicate for 30 minutes prior to injection.

1.2.3. Inject mice (intraperitoneal injection; IP) with 0.1 mL of tamoxifen solution (2 mg tamoxifen) for three consecutive days. Confirm GCaMP6f expression by genotyping and use mice 10 days after the first injection.

1.2.3.1. Genotype mice by clipping a small piece of ear from each animal. Then, use the HotSHOT method[55] for genomic DNA isolation by incubating ear clips at 95 °C for 60 minutes in 75mL of NaOH and then neutralizing by 75 mL of Tris buffer. Use standard PCR to determine genotype of each animal, 2 mL of DNA in a 20 mL reaction with GCaMP6f specific primers[56]. Run 10 mL of PCR product on a 2% agarose gel to determine wild type (297 bp) and mutant (~450 bp) bands.

2. Preparation of Tissues for Ca^{2+} Imaging

2.1. Anaesthetize mice by inhalation with isoflurane (4%, see **Table of Materials**) in a ventilated hood and then sacrifice by cervical dislocation.

2.2. Using sharp scissors open the abdomen of mice, remove the small intestine and place in Krebs-Ringer bicarbonate solution (KRB). Open the small intestine along the mesenteric border and wash away any intraluminal contents with KRB. Using sharp dissections, remove the mucosa and sub-mucosa layers.

NOTE: KRB solution has the following composition (in mM): NaCl 118.5, KCl 4.7, $CaCl_2$ 2.5, $MgCl_2$ 1.2, $NaHCO_3$ 23.8, KH_2PO_4 1.2, dextrose 11.0. This solution has a pH of 7.4 at 37 °C when bubbled to equilibrium with 95% O_2- 5% CO_2.

2.3. Using small pins, pin the small intestine tissue to the base of a 5 mL volume, 60 mm diameter Sylgard-coated dish with the circular smooth muscle layer facing up. Perfuse the preparation with warmed KRB solution at 37°C for an equilibration period of 1 hour before experimentation.

2.4. Following this equilibration period, perform *in situ* Ca^{2+} imaging of small intestinal ICC-MY and ICC-DMP using confocal microscopy (the images in this protocol were acquired with a confocal microscope fitted with a spinning-disc). Due to the benefits of GECIs described above, use high-resolution time-lapse images (>30 frames per second, FPS) combined with high power objectives (60-100X) to acquire movies of dynamic Ca^{2+} signals in ICC.

NOTE: To reduce tissue movement, apply nicardipine (0.1-1 µM) during recordings as described previously[37–41].

2.5. Distinguish ICC-MY and ICC-DMP in the small intestine using their differing anatomical location, morphology and basal Ca^{2+} activity patterns.

2.5.1. Locate ICC-MY at the level of the myenteric plexus, between the circular and longitudinal smooth muscle layers of the small intestine. They are stellate shaped, forming a connected network (**Figure 3A**). CTCs (described above) propagate through the network of ICC-MY with a regular occurrence of ~ 30 cycles per minute.

2.5.2. Conversely, locate ICC-DMP in a single plane at the level of the deep muscular plexus, in between the circular smooth muscle layer and the submucosal plexus. ICC-DMP do not form a network and are spindle shaped cells (**Figure 2A**) that exhibit no regular propagating events and instead fire stochastic, localized intracellular Ca^{2+} transients.

2.6. Regardless of the acquisition software utilized, save movies as a stack of TIFF images.

3. Analysis of Stochastic Ca^{2+} Signals in ICC-DMP using Spatio-Temporal Mapping (STM)

3.1. Analyze ICC-DMP using spatio-temporal mapping with a combination of ImageJ software (NIH, USA, free to download at http://imagej.nih.jov/ij) and custom made software (Volumetry, version G8d, GWH, operable on Mac OS, contact Grant Hennig grant.hennig@med.uvm.edu regarding inquires for Volumetry access and use)

NOTE: An alternative approach to fully analyze these spatio-temporal maps with ImageJ alone is also provided in later sections (beginning at step 3.9).

3.2. Open Volumetry and use right mouse clicks to open folders containing movie files. Left click on the movie file to be analyzed to open it in Volumetry (must be in uncompressed TIFF format). Once opened, the movie will be contained within a blue-bordered window (Movie Window) that will encompass a large area of the right-hand screen. The left-hand side of the screen will contain the Plot Window (upper 4/5ths) and the Traces Window (lower 1/5th).

3.3. Adjust the dimensions of the movie by holding down SHIFT and simultaneously scrolling up with the middle mouse button (MMB, reduces size) or scrolling down with the MMB (increases size). Initiate or stop playback by pressing 'A'; the speed of playback can be adjusted by pressing the up and down arrow keys.

3.4. To create a STM using Volumetry, draw an ROI over an entire cell by holding down SHIFT while clicking and dragging the left mouse button. Adjust the orientation of the ROI by scrolling with the MMB at the corners of the ROI. When the ROI is in place over the cell to be analyzed (**Figure 2A**), use right clicks in the Movie Window to access 'ROI STMs – STMyAvg>xRow' and left click to create an STM of the cell activity in the Plot Window (there is also an option to select 'STMxAvg>yRow', which one is selected will depend on whether the orientation of the cell is more aligned with the x or y axis, for example the cell highlighted **Figure 2A** is more orientated on the y axis').

3.5. Left click on the STM in the Plot Window and press 'P' to subtract average background noise and press 'H' to increase the contrast of the STM. Save the STM by right clicking on it to access 'STM Load Save- Save STM as .tif' and then left clicking to save as a TIFF.

3.6. The remainder of the analysis of ICC-DMP will be carried out in ImageJ. ImageJ consists of two main components, a toolbar with a fixed position on the top of the monitor and a mobile user interface. Using ImageJ, open the STM TIFF file of ICC-DMP Ca^{2+} activity (File-Open on the Image J toolbar).

3.7. Open the Volumetry created STM, which will have time vertically orientated. ImageJ will automatically open TIFF files as either RGB or 16-bit images. To improve image quality, left click 'Image' in the ImageJ toolbar. Scroll on the first option 'Type' to reveal a drop down menu of various image formats, scroll over '32-bit', and left click to change.

3.8. To make the STM readable against time from left to right, left click on the ImageJ toolbar on the following path: 'Image-Transform-Rotate 90 Degrees Left'. It is also possible to create STMs of *in situ* Ca^{2+} activity using linescans with ImageJ alone without Volumetry and this is detailed below.

NOTE: Once the STMs are created, they are analyzed in the same way regardless of which software was used to generate them. To skip this alternative method for creating STMs in ImageJ, skip to step 3.19.

3.9. To create STMs with ImageJ, open the stack of TIFF files that make up the recording of ICC-DMP Ca^{2+} activity (File-Open on the Image J toolbar). ImageJ will automatically open TIFF files as either RGB or 16-bit images. To improve image quality, left click 'Image' in the ImageJ toolbar. Scroll on the first option 'Type' to reveal a drop down menu of various image formats, scroll over '32-bit', and left click to change.

3.10. Background noise (resulting from auto fluorescence or camera noise) should now be subtracted from the movie. Left click the 'Rectangular Selection' function in the ImageJ interface and draw an ROI (by left clicking and dragging to desired size and shape) over the background fluorescence of the movie.

3.11. After selecting the ROI, left click on 'Analyze' in the ImageJ toolbar, and then left click 'Histogram' from the resulting dropdown menu. A pop-up box will then appear inquiring about pixel range values to calculate; ImageJ has the values of the ROI preselected so left click 'OK'.

3.12. After clicking 'OK', a new pop-up box containing a histogram will appear showing the distribution of values for the pixel noise of the background within the ROI. Take note of the mean value listed below the histogram and then close the pop-up box.

3.13. Click back to the 32-bit movie and select the entire FOV by left clicking 'Edit' on the ImageJ toolbar, scrolling to 'Selection', and left clicking on 'Select All' from the revealed dropdown menu.

3.14. Left click 'Process' on the ImageJ toolbar, scroll to 'Math' and left click 'Subtract' from the revealed dropdown menu.

3.15. A popup box will appear where a value to be subtracted from the FOV can be inserted. Enter the mean value acquired from the histogram in step 3.12 above and click 'OK'. ImageJ will then ask to process all the frames in the TIFF stack (and not just the single frame the movie is currently on). Click 'Yes'.

3.16. After clicking 'Yes', the movie will turn black. To correct this, left click 'Image' in the ImageJ toolbar and scroll over 'Adjust'. Left click on the revealed first option for 'Brightness/Contrast' (B&C). This will bring up a pop up box where various aspects of brightness and contrast may be modified. Left click on the 'Auto' option once to reveal the increased quality in the movie. Leave this B&C pop up box open for future use.

3.17. To create a linescan, first right click on the line selection tool in the ImageJ interface to reveal options for different lines; left click on 'Segmented Line' to choose it from the list. With the 'Segmented Line' tool selected, use single left clicks to draw a line along the mid axis of an individual ICC-DMP. Each single left click will fix the line at that particular point and the line can then be freely moved further at any desired angle. When the line is completed, double left click to fix the line in place.

3.18. Left click 'Image' on the ImageJ toolbar and scroll over 'Stacks' and left click on the 'Reslice' option. A popup box will appear; left click on the option to 'Rotate 90 Degrees', this will orientate the linescan from left to right so that it can be calibrated and read against time on the x-axis, with space on the y-axis. Click 'OK' to create the STM.

3.19. The intensity of the STM will be created on a greyscale with high intensity Ca^{2+} signals shown as varying degrees of white, off white or light gray depending on their intensity. Normally, the contrast of the created linescan will need to be improved. Do this by clicking 'Auto' on the B&C pop up box.

3.20. The intensity of the fluorescence of the linescan is presented on the STM in arbitrary pixel values. In order to accurately measure the amplitude of Ca^{2+} signals from the STM, the

fluorescence values of the STM (F) now need to be normalized. Using the 'Rectangular Selection' function in the ImageJ interface, draw an ROI on an area of the STM that displays the most uniform and least intense area of fluorescence (F_0).

3.21. Repeat the steps taken in 3.11 – 3.12 to obtain a mean value (F_0) of the intensity within the selected ROI and then select the entire STM by left clicking on 'Edit-Selection-Select All' from the ImageJ toolbar.

3.22. Left click 'Process' on the ImageJ toolbar and scroll to 'Math'; left click 'Divide' from the revealed options. In the subsequent popup box, enter the mean value (F_0) obtained from step 3.21. Upon dividing the entire STM by (F_0) the STM will turn black; correct this by clicking 'Auto' on the B&C pop up box. The linescan is now calibrated for amplitude, with intensity of fluorescence expressed as F/F_0.

3.23. The STM will currently display the number of frames in the TIFF stack on the x-axis and the number of pixels representing the length of the cell on the y-axis. In order to quantify temporal and spatial information from Ca^{2+} signals, calibrate the STM for space and time. Left click 'Image' in the ImageJ toolbar and left click 'Properties'. A popup box will appear. Within this window, enter the appropriate values to fully calibrate the STM.

3.24. For 'Pixel Width', enter the length of time it takes to capture a single frame in seconds. For examples, at 5 FPS, enter a value of 0.2, for 50 FPS enter a value of 0.02, for 33 FPS enter a value of 0.033 *etc.* For 'Pixel Height', enter how many microns each pixel represents (will depend on the objective used and camera used for acquisition). 'Voxel Depth' is left at 1 before clicking 'OK'. No other parameters need to be adjusted within the window.

NOTE: After clicking 'OK', the STM will be fully calibrated for amplitude, space and time. Amplitude on the STM will be expressed as F/F_0, time on the x-axis will be expressed in seconds and space on the y-axis will be expressed in µm (**Figure 2B**). Ca^{2+} events on the STM are now ready to be measured, the calibrated STM can also be saved as a single TIFF image to analyze at a later date.

3.25. ImageJ has a number of built in color coded lookup table (LUTs) that may be used to color code the STM. Apply a built in LUT by left clicking on the ImageJ toolbar on the path 'Image-Lookup Tables' and choose an LUT to apply. Custom made LUTs can also be imported to the STM by left clicking on the ImageJ toolbar on the path 'File-Import-LUT' and then selecting the LUT to import. For example the STM shown in **Figure 2C** has had the custom LUT 'QUBPallete' (Queens University Belfast, UK) applied to it, to code warm colors (red, orange) as areas of intense Ca^{2+} fluorescence and cold colors (black, blue) as areas of low Ca^{2+} fluorescence.

3.26. To insert an amplitude calibration bar to indicate the range of amplitudes represented by the various colors, left click 'Analyze' from the ImageJ toolbar, scroll to 'Tools', and select 'Calibration Bar' from the revealed menu. Options are given for the size, zoom, range and position on the STM for the calibration bar; adjust these settings as desired and click 'OK'. Note that when

the calibration bar is inserted, ImageJ creates a new STM containing it, leaving the original version without the calibration bar intact and separate.

NOTE: If the 'Overlay' box is ticked when inserting the calibration bar, a new STM will not be generated.

3.27. To begin analyzing individual Ca^{2+} events, left click on the 'Straight Line' selector on the ImageJ interface. By initially left clicking on the STM, draw a straight horizontal line through the center of a Ca^{2+} event parallel to the x-axis (against time). Complete the line by left clicking a second time (**Figure 2D**).

3.28. Click 'Analyze' on the ImageJ toolbar and left click on 'Plot Profile'. A new box will appear with the plot profile of the Ca^{2+} event (**Figure 2E**).

NOTE: The 'List' option within this box will generate a list of XY values of the generated plot, which can be copied into a spreadsheet program to create traces if so desired.

3.29. To measure the amplitude of the Ca^{2+} event represented in the plot profile, left click on the 'Straight Line' selector on the ImageJ interface. Then, draw a vertical line from the baseline of the plot profile to the peak of the Ca^{2+} event; the length of the line (shown on the ImageJ interface) will represent the amplitude of the event expressed as $\Delta F/F_0$ (**Figure 2E**).

3.30. Using the acquired amplitude value, the duration of the Ca^{2+} event can be measured by drawing a straight line across the width of the event at the point of 50% maximum amplitude (full duration at half maximum amplitude, FDHM) or the full duration of the event may be measured if desired (**Figure 2E**).

NOTE: Experimenters will need to design specific criterion for thresholding valid Ca^{2+} events in these recordings. In our experiments, Ca^{2+} events were designated as being valid for analysis if its amplitude was >15% of the maximum amplitude event in the control section of recording. However, these thresholds will depend on the specific tissues and cells under study and are only arbitrary guidelines that require specific optimization for every type of tissue and cell.

3.31. By drawing a line along the upstroke or downstroke of the Ca^{2+} event plot profile, the rate of rise or fall may be calculated accordingly. After the line is drawn, the mouse cursor can be moved to the point where the line begins and where it ends. When the cursor is stationary over these points, x,y coordinates for this location will be displayed in the lower left side of the ImageJ interface. Thus, by acquiring x,y values for where the line begins (x_1,y_1) and ends (x_2, y_2), the rate of rise or fall ($\Delta F/s$) can be calculated as the slope of the line, $y_2 - y_1 / x_2 - x_1$ (**Figure 2F**).

3.32. In order to calculate the propagation or spatial spread of a Ca^{2+} event, left click on the 'Straight Line' selector on the ImageJ interface. Then, draw a straight vertical line along the length of the Ca^{2+} event along the y-axis. The length of the line (shown on the ImageJ interface) will represent the spatial spread of the event expressed as µm (**Figure 2G**).

3.33. Determine the velocity of a propagating Ca^{2+} event by drawing a line along the propagating front of the event and calculating the slope of the line. This may be performed manually in a similar manner described in step 3.32, by determining x,y values for where the line begins (x_1,y_1) and ends (x_2, y_2); these values will be displayed in the lower left side of the ImageJ interface when the mouse cursor is situated on the STM.

3.34. Upon the collection of the desired parameters for Ca^{2+} event quantification, pool these values average to generate mean values for each parameter on a per cell basis; alternatively, place all of the raw values in a distribution histogram to show their range (**Figure 2H**).

4. Quantification of CTCs in ICC-MY using Particle Based Analysis

4.1. Before analyzing movies in Volumetry with PTCLs, the spatial and temporal calibration of the movie will need to be inserted into the file name. Edit all files to be analyzed in Volumetry to contain within the title the number of seconds that each frame equals and also the number of microns that each pixel equals separated by a single dash, with the values encased in square brackets. For example, a movie acquired at 33 FPS with a 60X objective (512 x 512) should have [0.22-0.033] inserted into its file name.

4.2. Open Volumetry and use right mouse clicks to open folders containing movie files. Left click on the movie file to be analyzed to open it in Volumetry (**Figure 3A**, must be in uncompressed TIFF format).

4.3. In order to accurately calculate Ca^{2+} signals from the entire FOV, the movie will first undergo differentiation and smoothing to remove background interference (camera noise, auto fluorescence *etc.*) and increase the signal to noise ratio. In the Movie Window, right click to bring up a menu and using right clicks access 'STK Filter-Differentiate', right click again to input a value to differentiate, press ENTER, and left click to apply (for movies acquired at 33 FPS a value of 2 (Δt = ± 66-70 msec) works well, the value is increased as the rate of image capture increases).

NOTE: Differentiation in this context will reduce the intensity of areas of recording (pixels) that show no dynamic activity over the number of frames specified. Thus, if a value of '2' is inserted, each pixel in every frame of the recording is analyzed and if within that frame there is no dynamic change in pixel fluorescence 1 frame before and 1 frame after, the intensity within those pixels will be subtracted from the recording. Thus, non-dynamic background noise is removed and signal to noise is increased.

4.4. Smooth the differentiated movie by applying a Gaussian filter. Right click in the Movie Window to bring up a menu and using right clicks access 'STK Filter-Gauss KRNL', right click again to insert a value (always use an odd number, for movies acquired at 33 FPS, a value of 5 works well, 1.5 x 1.5 µm, StdDev 1.0) input a value, press ENTER, and left click to apply (**Figure 3B**).

4.5. Start to create PTCLs by first selecting a period of the movie that includes a quiescent period (20-40 frames) followed by the occurrence of a CTC and also 20-40 frames after the CTC. To do this, scroll through the movie by using the MMB to scroll left to right on the yellow bar.

4.6. With the selection made, use right clicks in the Movie Window to access 'STK Ops – Ramp DS PTCLinfo' and left click to apply. This function runs a PTCL analysis routine that progressively ramps the threshold from maximum intensity to minimum intensity. This will be displayed graphically in the Plot Window as a plot of noise and also in the Traces Window as three colored traces, with the green trace showing the number of PTCLs, the red trace showing average PTCL size, and the blue trace showing the absolute intensity threshold.

NOTE: The number and average size of PTCLs at each threshold is automatically calculated and then a semi-manual threshold is applied using the intensity at which at which the average size of PTCLs begins to drop, which occurs at the inflection point of the red trace in the Trace Window (**Figure 3D**, *i.e.* due to large numbers of spatially limited noise PTCLs reducing the average size of PTCLs).

4.7. Within the Plot Window, press 'H' to histogram balance the plot shown of PTCL noise. Cycle through color schemes by pressing '[' until the background is colored white with colored traces on top.

4.8. Press 'F' to bring up a measuring tool and left click on the plot at the intersection where the colored plots shift to the right hand side. This will mark a single vertical line in the scroll bar of the Traces Window below.

4.9. Within the Trace Window, scroll the MMB left to right from the inflection point of the red trace until the marked white vertical line created in step 4.10 and making sure that the blue trace is selected by right clicking on it, read off the 'yAVG' that will be displayed in the lower left hand side of the Traces Window. Deselect the selection by pressing the MMB once inside the Traces Window.

4.10. Within the Movie Window, press 'C' to bring up a color wheel, then press 'D' to adjust threshold. Valid PTCLs will now be shown as red in the Movie Window (**Figure 3C**) and those that saturate will be white. Remove the white areas by scrolling up with the left mouse button.

4.11. Scroll up or down with the MMB to adjust the yellow numerical value in the color wheel, adjust this value to the yAVG value taken from step 4.11. This will assign everything in red as an active Ca^{2+} transient PTCL at the determined threshold point. To save this as a coordinate based particle file, use right clicks to access 'STK 3D-Save PTCLS 0' and then left click to save the file.

4.12. Quit Volumetry and reopen. Open the PTCL file (.gpf file) created in step 4.13. In this file type, all active Ca^{2+} transients are saved as a uniform blue PTCL (**Figure 3E**). As each PTCL is an individual entity with its own ID, area and perimeter coordinates, state flags (see below) and

result arrays, the analysis of spatio-temporal characteristics of PTCLs, or between PTCLs is streamlined.

4.13. To begin PTCLs analysis, remove any remaining PTCL noise (small invalid PTCLs created when the .gpf file is generated) by using right clicks in the Movie Window to access 'PTCL STKOPS-Flag ptcls >Min=70' and left click to apply. This action will flag PTCLs greater than 6 μm^2 (~diameter > 2µm) and Volumetry will assign them to 'FLAG 1' selection. When this is complete, PTCLs that are above this threshold (FLAG 1) will appear as a light purple color in the Movie Window, whereas any PTCLs below threshold will remain their base blue color (**Figure 3F**).

4.14. Create heat map representations of PTCL activity by using right clicks in the Movie Window to access 'PTCL STKops-StatMap Flag='. By right clicking on this final path, a flag assignment to analyze can be entered. Thus, if wishing to quantify the PTCLs assigned to FLAG1, simply enter '1', press ENTER and then left click to apply. This will generate a heat map showing the total PTCLs for the entire length of recording, with different colors representing occurrence (%) throughout the recording (**Figure 3G**, warm colors indicate increased occurrence at that location).

4.15. Save heat maps by right clicking on them to access 'STM Load Save- Save STM as .tif' and then left clicking to save as a TIFF.

4.16. Quantify PTCL activity by using right clicks in the Movie Window to access 'PTCL Measure-PTCLStats STK =', by right clicking on this final path, a flag assignment to analyze can be entered. Thus, if wishing to quantify the PTCLs assigned to FLAG1, simply enter '1', press ENTER and then left click to apply. This will generate a series of traces in the Trace Window.

4.17. Volumetry will by default superimpose the PTCL traces generated in step 4.17 on top of each other. Separate them using right clicks in the Trace Window to access 'Align-Separate Trace' and left click to apply. This will reveal the four different PTCL traces that quantify the Ca^{2+} PTCL activity in the movie showing PTCL area (green), PTCL count (red), PTCL size (cyan), and PTCL size standard deviation (blue) plotted against time (**Figure 3H**).

4.18. These traces may be saved as a text file that can be imported into a spreadsheet program for further analysis. To save traces, hold down SHIFT and use right clicks in the Trace Window to access 'Assorted-Dump ROI as Text' and left click to save the file. This information is then collected and illustrated in histograms or other appropriate graphical representations (**Figure 3H**).

4.19. In order to look at the initial occurrence of PTCLs (*i.e.,* to look at firing sites), these initial PTCLs are given a different flag assignment. To better isolate firing sites occurring within the network, only those PTCLs that did not overlap with any particles in the previous frame but overlap with particles in the next 70 ms are considered firing sites.

4.20. To apply this threshold, use right clicks in the Movie Window to access 'PTCL Behaviour-F1 InitSites>F=3' and left click to apply. This will assign initiating PTCLs as 'FLAG 3', and PTCLs that meet this criteria will now appear as a lime green color in the movie (**Figure 4A**).

4.21. Volumetry also affords the ability to quantify and plot the number of PTCL firing sites in a given FOV as well as plotting their probability of firing during a CTC. To analyze these parameters, create a heat map of initiating PTCLs (FLAG 3) as described in step 4.16 (**Figure 4B**).

4.22. Left click in the Plot Window and then press 'C' to bring up a color wheel and press 'D' to threshold. The heat map of initiating PTCLs will then turn grey and white. Remove all white by scrolling up with the left mouse button and threshold the PTCLs in the heat map so that only valid PTCLs are covered in grey (adjust threshold by scrolling up and down with the MMB).

4.23. Use right clicks over the heat map in the Plot Window to access 'STM PTCLs-Find PTCLs 70' and left click to apply. This will assign all grey PTCLs in the map that are greater than 70 pixels^2 in size to be allocated as a separate color coded initiation PTCL or PTCL firing site (**Figure 4C**).

4.24. Plot the activity of each of these firing sites against time by right clicking on the PTCL firing map and accessing 'STM PTCLs-Create PTCL rois' and left clicking to apply. This will generate a new image in the Movie Window with all the separate colored PTCL firing sites displayed with an ROI around them.

4.25. Use right clicks in the Movie Window to access 'PTCL Measure-PTCLpixROIBM>=1' and left click to apply. This will identify all ROIs in the Movie Window that contain at least one PTCL and will plot all of the activity within these ROIs in the Traces Window. By default, these traces will be superimposed on one another. To separate them, use right clicks in the Trace Window to access 'Align-Separate Trace' and left click to apply. To save traces, hold down SHIFT and use right clicks in the Trace Window to access 'Assorted-Dump ROI as Text' and left click to save the file.

4.26. The activity of each firing site can also be plotted as an occurrence map. To do this, use right clicks in the Movie Window to access 'PTCL Measure-ROI Pianola=10' and left click to apply. This will generate a plot of all the firing sites against time in the Plot Window. Each firing site will be displayed as a separately colored entity, each in its own 'lane' and these plots correspond to Ca^{2+} PTCLs initiating during CTCs (**Figure 4D,E**) Save these occurrence maps by right clicking on them to access 'STM Load Save- Save STM as .tif' and then left clicking to save as a TIFF.

4.27. To quantify the probability of firing at each firing site during a CTC, use right clicks in the Movie Window to access 'PTCL Behaviour-Mark IS =1' and left click to apply. This will identify all frames in the movie that contain PTCLs above threshold and these will be marked in the bottom of the Movie Window as vertical blue lines.

4.28. CTCs manifest as rapid clustering of asynchronous firing from multiple firing sites within the FOV with ~1 s gaps in between each CTC cycle. This regularity and long gap of no active PTCLs between CTCs is used to further define a CTC for analysis.

4.29. Use right clicks in the Movie Window to access 'PTCL Behaviour-Block IS Gap<=', and use a right click on the final point to enter a number. This command will group the active PTCL frames identified in step 4.28 into blocks and blocks are based on the number of frames that separate active PTCLs. For recordings of 33 FPS for example, a value of 10 works well. If active PTCLS are less than 10 frames apart (330 ms) they are grouped into a single block for analysis (the blocks are then shown as pink rectangles over the vertical blue lines at the bottom of the Movie Window, with each pink rectangle now indicating a CTC).

4.30. Use right clicks in the Movie Window to access 'PTCL Measure-PTCL Event Prob'. This will generate a text file that can be imported into a spreadsheet program. This text file will provide a vast quantity of data on the nature of the initiation sites that were defined from steps 4.16-4.23 and their contribution to CTCs.

NOTE: The text file will show the number of initiation sites (referred to as 'domains'), the size of the site in pixels and μm^2, probability of each initiation site firing either once or multiple times during each CTC (given as a%), the average duration and size of PTCLs occurring at that initiation site, the number of CTC cycles (as defined in step 4.23) and the percentage of firing sites that fired during each CTC cycle. This information is collected and illustrated in histograms or other appropriate graphical representations (**Figure 4F**).

Representative Results:

Using Kit-Cre-GCaMP6F mice (**Figure 1**), dynamic Ca^{2+} signaling behaviors of ICC in the gastrointestinal tract can be imaged *in situ*. With confocal microscopy, high-resolution images of specific populations of ICC can be acquired without contaminating signals from other populations of ICC within the same tissue but in anatomically distinct planes of focus (**Figure 2A**) [37, 39–41]. It is possible to record brief (<100 ms), localized Ca^{2+} events that were not possible with membrane permeable Ca^{2+} indicators. Spatio-temporal mapping with Volumetry or ImageJ software can be used to generate STMs of all Ca^{2+} events within cells *in situ*. Using this approach, Ca^{2+} events in an entire FOV can be visualized and mapped (**Figure 2B,C**), rather than just recording the limited activity of a single ROI. These methods can be extended to each cell within a given FOV, ensuring representative data collection from all cells and providing quantitative information about relative amplitudes, transient durations, rate of rise and fall of transients, *etc.* (**Figure 2E,F**). STM analysis, as opposed to ROI-based intensity plots, also provide the ability to monitor and record spatial characteristics of Ca^{2+} signaling, such as spatial spread and propagation velocity, as shown in **Figure 2G**. This information can be amassed to provide a rather complete view of Ca^{2+} signaling behaviors in cells in their native environments (**Figure 2H**).

PTCL analysis can be used to quantify more complex Ca^{2+} signaling behaviors, such as those occurring within interconnected cellular networks. An example of this application is provided by the analysis performed on ICC-MY (**Figure 3A**). Usually in such complex preparations, background noise and signal to noise can be an issue. However, using Volumetry software to apply differential and smoothing filters on movies of Ca^{2+} activity and then applying noise threshold protocols to filter out noise (**Figure 3B-D**) background noise can be removed from complex recordings of

dynamic activity. Using PTCL analysis such as those shown in **Figure 3E-G**, quantitative information about Ca^{2+} signaling can be calculated by measuring the PTCL area, PTCL count and PTCL size which indicate spatial ranges of activation of Ca^{2+} signals in a FOV. These data can be compiled as shown in **Figure 3H** and analyzed statistically, as appropriate. **Figure 4** illustrates how PTCL analysis allows in depth quantification of sub-cellular Ca^{2+} signaling by examining the location and firing probabilities of Ca^{2+} firing sites. By allocating PTCLs into different FLAGs based on their temporal characteristics, initiating PTCLs can be accurately mapped as shown in **Figure 4C-E** and a wealth of hard data acquired on the number of initiation sites (referred to as 'domains'), the size of the site in pixels and μm^2, probability of each initiation site firing either once or multiple times during each CTC (given as a%), the average duration and size of PTCLs occurring at the initiation site, the number of CTC cycles (as defined in step 4.23) and the% of firing sites that fired during each CTC cycle. These techniques allow a high level of data mining and quantification of *in situ* Ca^{2+} signals occurring within an intact cellular network that are not possible with ROI-based analyses.

Figure Legends:

Figure 1: Generation of KitGCaMP6f mice. Schematic diagram of how Ai95 (RCL-GCaMP6f)-D (GCaMP6f mice) were crossed with c-$Kit^{+/Cre\text{-}ERT2}$ (Kit-Cre mice) to generate Kit-Cre-GCaMP6f mice. These mice are injected with tamoxifen at ages of 6-8 weeks to induce Cre Recombinase and subsequent GCaMP6f expression exclusively in ICC.

Figure 2: Analysis of stochastic Ca^{2+} signals in ICC-DMP using spatio-temporal mapping (STM). (A) Representative image of several ICC-DMP from the small intestine of a Kit-Cre-GCaMP6F mouse *in situ.* A green ROI indicates the size and orientation of ROI to draw around a single ICC-DMP within the FOV to create an STM in Volumetry. **(B)** STM of Ca^{2+} activity in the ICC-DMP highlighted in panel A after it has been properly calibrated for amplitude, space and time. **(C)** The same STM shown in panel B after it has been color coded with a lookup table (QUBPallete). **(D)** Expanded image of ICC-DMP Ca^{2+} transients displayed on a color coded STM, indicating where to draw a line through a Ca^{2+} event across its time (x) axis to create a plot profile of its activity in ImageJ. **(E)** Plot profile of the Ca^{2+} event highlighted in panel D, indicating where lines shown be drawn to accurately measure the amplitude and duration of the event. **(F)** Plot profile of the Ca^{2+} event highlighted in panel D, indicating where lines shown be drawn to accurately measure the rate of rise and rate of fall of the event. **(G)** Expanded image of ICC-DMP Ca^{2+} transients displayed on a color coded STM, indicating where to draw a line through a Ca^{2+} event across its space (y) axis to accurately measure its spatial spread. **(H)** Representative histograms of pooled data from ICC-DMP illustrating how to graphically display the amplitude, duration, and spatial spread values acquired from following the above steps.

Figure 3: Quantification of CTCs in ICC-MY using particle based analysis. (A) Representative image of an ICC-MY network from the small intestine of a Kit-Cre-GCaMP6F mouse *in situ.* **(B)** Image taken from the recording shown in panel A after it has undergone a differential filter of Δt = ±66–70 ms and a Gaussian filter of 1.5 × 1.5 µm, StdDev 1.0. **(C)** Image taken from the video in B after thresholding was completed with PTCLs above threshold shown in red. **(D)** Traces of PTCL count and mean PTCL size in a thresholding protocol to eliminate noise in the movie shown in

panel B. PTCLs were created using a flood-fill algorithm that marked the structure of all adjoining pixels that had intensities above threshold, Ca^{2+} transient PTCLs were larger than noise PTCLs. The threshold at which large numbers of small sized noise PTCLs emerged and began to reduce the mean size of PTCLs can be used as a common threshold for all recordings. **(E)** Representative image from the coordinate-based Ca^{2+} PTCL file created from the thresholded recording in C. **(F)** Representative image taken from the PTCL file of E after a screening criteria of >6 μm^2 (diameter ~2 µm or smaller) was applied; PTCLs above this limit are flagged (FLAG 1) as light purple particles and considered valid PTCLs. **(G)** Heat map showing the total PTCLs (FLAG 1) for the entire recording of the video shown in panel F, with total PTCLs summated with colors representing occurrence throughout the recording (warm colors indicate increased occurrence at that location). **(H)** Representative traces of PTCL area (blue) and PTCL count (red) derived from the PTCL file created in panel A-G. Representative histograms of pooled data from several experiments are shown below the traces.

Figure 4: Analysis of Ca^{2+} firing sites in ICC-MY using particle based analysis. (A) Representative image taken from the PTCL file of **Figure 3E** after FLAG 1 PTCLS are further refined into FLAG 3, the flag status for Ca^{2+} firing sites. FLAG 3 PTCLs are displayed as lime green (only those PTCLs that did not overlap with any particles in the previous frame but overlap with particles in the next 70 ms were considered firing sites). **(B)** Heat map showing the total PTCLs (FLAG 3) for the entire recording of the video shown in panel A, with total PTCLs summed with colors representing occurrence throughout the recording (warm colors indicate increased occurrence at that location). **(C)** Representative map of Ca^{2+} firing sites shown in panel B, with each different firing site allocated a different identifying color. **(D)** Representative traces of PTCL area (blue) and PTCL count (red) derived from the PTCL file created in **Figure 3A-G**. **(E)** An occurrence map of the activity of individual firing sites. Each firing site within the FOV is displayed as a colored block in its own 'lane' against time. **(F)** Representative histograms of pooled data from several experiments are shown illustrating values accumulating for Ca^{2+} firing site firing probability / CTC and the number of Ca^{2+} firing sites in a FOV.

Discussion:

Ca^{2+} imaging of specific types of cells within intact tissues or within networks of cells often reveals complex patterns of Ca^{2+} transients. This activity requires careful and in-depth analyses and quantification to capture as much information about the underlying events and kinetics of these events as possible. STM and PTCL analysis provide an opportunity to maximize the amount of quantitative data yielded from recordings of this type.

The narrow, spindle shaped morphology of ICC-DMP make them well suited to STM analysis derived from the STMs outlined above. However, this analysis is not well suited to ICC-MY that are stellate shaped and connected in a network (**Figure 3A**). Furthermore, the Ca^{2+} signaling patterns in ICC-MY are more complex, manifesting as propagating CTCs from multiple sites of origin throughout the ICC-MY network. Thus, in order to quantify the activity occurring in the entire ICC-MY network within a FOV, particle (PTCL) analysis was implemented using custom made software (Volumetry, version G8d, GWH, operable on Mac OS, contact Grant Hennig grant.hennig@med.uvm.edu regarding inquires for Volumetry access and use).

742
743 STM analysis allows all Ca^{2+} events within single cells and within all of the cells in a FOV to be
744 analyzed critically across a range of spatial and temporal parameters. The protocol described
745 illustrates how these techniques can be applied to ICC-DMP of the mouse small intestine. By fully
746 quantifying Ca^{2+} signaling in ICC-DMP, as shown in **Figure 2B**-G, Ca^{2+} signaling patterns have been
747 characterized in detail[37]. These analyses have been applied to recordings where ICC-DMP
748 undergo interventions to finely quantify the effects of blocking or stimulating Ca^{2+} release / Ca^{2+}
749 influx / neurotransmission pathways[37,39–41]. These techniques can be easily applied to other intact
750 tissue preparations. For example, STM analysis as described here has been utilized to identify
751 new mechanistic pathways involved in the generation of intracellular Ca^{2+} waves recorded in
752 urethral smooth muscle *in situ*[57].
753
754 The preparation of STMs in Volumetry requires some caution, as the function in Volumetry that
755 creates the STM from the drawn ROI (**Figure 2A**) is an average value of intensity. Thus, the
756 amplitude of Ca^{2+} signals could potentially be diluted if the ROI is drawn wider or longer than the
757 Ca^{2+} event or cell of interest. Thus, users should be careful to draw ROIs that are as tightly fitting
758 as possible to the Ca^{2+} signals or particular cell that they are analyzing in order to alleviate this
759 issue. Similarly, creating STMS using single pixel linescans in ImageJ means that accurate mapping
760 of Ca^{2+} events is subject to the proximity of the Ca^{2+} signal to the drawn line. Such concerns are
761 minor in thin spindle shaped cells such as ICC-DMP, however other cell types with a more stellate
762 or round morphology may make this type of analysis inappropriate to map all Ca^{2+} signals
763 accurately. When preparing STMs for analysis, regardless of whether they were made in
764 Volumetry or with ImageJ linescans, there are a few areas to be highlighted for troubleshooting
765 purposes. It is important to change the image quality to 32-bit before performing any calibration
766 on the STMs. Failure to do so, or doing so after calibrating for F/F_0 can lead to inconsistent
767 measurements across experiments. Always check the image quality of the STM, which is stated
768 in the top area of the white border of the STM itself when opened with ImageJ. Another potential
769 area of inconsistency is selecting the F_0 value when calibrating for amplitude. It is vital that for
770 selecting the region for F_0, that it covers an area of the cell that is uniform and in focus. For this
771 reason, areas of the cell that have an unstable basal fluorescence or that change due to
772 movement or other artefacts are not ideal and rigorous motion stabilization protocols should be
773 employed in these cases.
774
775 Within *in situ* or cultured preparations containing interconnected cellular networks, such as ICC-
776 MY in the small intestine, PTCL analysis provides a streamlined technique to quantify complex,
777 subcellular Ca^{2+} events occurring in the network. Moreover, it also allows all Ca^{2+} events in the
778 network within a given FOV to be analyzed, rather than using arbitrary ROIs, which only provide
779 information on frequency and intensity within the ROI. An advantage of the PTCL analysis
780 described here is that by applying differential and Gaussian smoothing filters to recordings, a
781 large amount of noise can be removed from movies that may contain contaminating light from
782 cells not of interest or due to non-dynamic bright spots or inclusions. It is important to note that
783 the amount of differentiation applied to recordings will depend largely on the acquisition rate
784 used by the experimenter. Differentiating movies as described in the protocol provides a means
785 of applying a filter to the movie to remove high frequency noise from recordings. Applying a

differentiation value of '2' when acquiring at 33FPS works well to remove background noise while maintaining good signal to noise (if the value is too low, noise will be picked up but signal to noise will be compromised if the value is too high). The differentiation value applied should be increased with faster acquisition rates, for example at 100 FPS, a differentiation value of '7' gives approximately the same signal to noise ratio as a value of '2' to a 33FPS recording. Experimenters will need to optimize these settings accordingly for their preparations and recording conditions.

The thresholding protocol described in **Figure 2D** allows a consistent thresholding procedure to be applied to different recordings made on different systems with different acquisition software. This flexibility allows data from multiple investigators working on different systems to compile their recordings into the same datasets. By using the FLAG system in Volumetry, PTCL analysis allows the visualization and quantification of individual Ca^{2+} firing sites within a network in detail. Information can be gathered on the number of initiation sites, the size of the site in pixels and μm^2, and the average duration of PTCLs occurring at that site. This PTCL analysis allowed the first characterization of CTC activity in the small intestine at a sub-cellular level, and, using the different FLAGs in Volumetry software, PTCLs at both the network and individual firing site level were quantified in intact tissue preparations from Kit-Cre-GCaMP3 mice[38]. From these initial observations, this analysis has been further utilized to study novel Ca^{2+} influx pathways in GI ICC-MY such as store-operated-Ca^{2+}-entry[42] and the role of mitochondrial Ca^{2+} signalling on GI pacemaking[41]. Much like STM analysis described above, PTCL analysis can be easily adapted to different intact preparations other than that described in this protocol. For example, a recent study used PTCL analysis to study novel rhythmic Ca^{2+} events occurring in the intact cellular networks of the lamina propria of the rat urinary bladder[58,59] and thus could be easily applied to other complex, intact cellular systems such as neuronal systems. While this paper focused on Ca^{2+} imaging in intact tissues with GECIs, these analysis techniques can also be run on isolated cells and tissues loaded with traditional Ca^{2+} indicator dyes. The STM based analysis has been used to successfully quantify localized Ca^{2+} signals and Ca^{2+} waves from spindle shaped interstitial cells and smooth muscle cells from a variety of preparations[11,60–63]. Furthermore, the PTCL analysis routines described here have also been applied to *in situ* network preparations visualized with Cal 520[58,59]. However, these studies also retain the disadvantages of such dye loading protocols such as ambiguous cell identification and problems with signal to noise.

The examples illustrated above demonstrate that both STM and PTCL analysis are highly malleable techniques that can be used to quantify complex Ca^{2+} signaling in a diverse range of intact tissue preparations. The approaches offer many benefits over traditional ROI based intensity plots that have been routinely used previously and should provide investigators with more valuable quantitative information on Ca^{2+} signaling than could be previously achieved.

Acknowledgements:
Funding was provided by the NIDDK, via P01 DK41315.

Disclosures:
The authors have nothing to disclose.

References:

1. Wellman, G.C., Nelson, M.T. Signaling between SR and plasmalemma in smooth muscle: Sparks and the activation of Ca2+-sensitive ion channels. *Cell Calcium*. **34** (3), 211–229, doi: 10.1016/S0143-4160(03)00124-6 (2003).
2. Mironneau, J., Arnaudeau, S., Macrez-Lepretre, N., Boittin, F.X. Ca2+sparks and Ca2+waves activate different Ca2+-dependent ion channels in single myocytes from rat portal vein. *Cell Calcium*. **20** (2), 153–160, doi: 10.1016/S0143-4160(96)90104-9 (1996).
3. Berridge, M.J. Inositol trisphosphate and calcium signalling mechanisms. *Biochimica et Biophysica Acta - Molecular Cell Research*. **1793** (6), 933–940, doi: 10.1016/j.bbamcr.2008.10.005 (2009).
4. Berridge, M.J., Lipp, P., Bootman, M. Calcium signalling. *Current biology*. **9** (5), R157-R159, doi: 10.1038/nrm1155 (1999).
5. Bootman, M.D. *et al.* Calcium signalling—an overview. *Seminars in Cell & Developmental Biology*. **12** (1), 3–10, doi: 10.1006/scdb.2000.0211 (2001).
6. Brain, K.L., Bennett, M.R. Calcium in sympathetic varicosities of mouse vas deferens during facilitation, augmentation and autoinhibition. *The Journal of Physiology*. **502** (3), 521–536, doi: 10.1111/j.1469-7793.1997.521bj.x (1997).
7. Berridge, M.J., Lipp, P., Bootman, M.D. The versatility and universality of calcium signalling. *Nature Reviews. Molecular Cell Biology*. **1** (1), 11–21, doi: 10.1038/35036035 (2000).
8. Dupont, G., Goldbeter, A. Problems and paradigms: Oscillations and waves of cytosolic calcium: Insights from theoretical models. *BioEssays*. **14** (7), 485–493, doi: 10.1002/bies.950140711 (1992).
9. Bootman, M.D., Berridge, M.J. The elemental principles of calcium signaling. *Cell*. **83** (5), 675–678, doi: 10.1016/0092-8674(95)90179-5 (1995).
10. Berridge, M.J., Dupont, G. Spatial and temporal signalling by calcium. *Current Opinion in Cell Biology*. **6** (2), 267–274, doi: 10.1016/0955-0674(94)90146-5 (1994).
11. Drumm, B.T. *et al.* The role of Ca 2+ influx in spontaneous Ca 2+ wave propagation in interstitial cells of Cajal from the rabbit urethra. *The Journal of Physiology*. **593** (15), 3333–3350, doi: 10.1113/JP270883 (2015).
12. Bayguinov, P.O., Hennig, G.W., Smith, T.K. Ca $^{2+}$ imaging of activity in ICC-MY during local mucosal reflexes and the colonic migrating motor complex in the murine large intestine. *The Journal of Physiology*. **588** (22), 4453–4474, doi: 10.1113/jphysiol.2010.196824 (2010).
13. Drumm, B.T., Sergeant, G.P., Hollywood, M.A., Thornbury, K.D., McHale, N.G., Harvey, B.J. The role of cAMP dependent protein kinase in modulating spontaneous intracellular Ca2+ waves in interstitial cells of Cajal from the rabbit urethra. *Cell Calcium*. **56** (3), 181–187, doi: 10.1016/j.ceca.2014.07.002 (2014).
14. Nathanson, M.H., Padfield, P.J., O'Sullivan, A.J., Burgstahler, A.D., Jamieson, J.D. Mechanism of Ca2+ wave propagation in pancreatic acinar cells. *Journal of Biological Chemistry*. **267** (25), 18118–18121 (1992).
15. Straub, S. V, Giovannucci, D.R., Yule, D.I. Calcium wave propagation in pancreatic acinar cells: functional interaction of inositol 1,4,5-trisphosphate receptors, ryanodine receptors, and mitochondria. *The Journal of General Physiology*. **116** (4), 547–560, doi:

10.1085/jgp.116.4.547 (2000).
16. Sneyd, J., Tsaneva-Atanasova, K., Bruce, J.*I.E.*, Straub, S. V., Giovannucci, D.R., Yule, D.I. A model of calcium waves in pancreatic and parotid acinar cells. *Biophysical Journal*. **85** (3), 1392–1405, doi: 10.1016/S0006-3495(03)74572-X (2003).
17. Jaggar, J.H., Porter, V.A., Lederer, W.J., Nelson, M.T. Calcium sparks in smooth muscle. *American Journal of Physiology. Cell physiology*. **278** (2), C235–C256, doi: 10.1152/ajpcell.2000.278.2.C235 (2000).
18. Nelson, M.T. *et al.* Relaxation of arterial smooth muscle by calcium sparks. *Science*. **270** (5236), 633–637, doi: 10.1126/science.270.5236.633 (1995).
19. Cheng, H., Lederer, W.J., Cannell, M.B. Calcium sparks: Elementary events underlying excitation-contraction coupling in heart muscle. *Science*. **262** (5134), 740–744, doi: 10.1126/science.8235594 (1993).
20. Parker, I., Choi, J., Yao, Y. Elementary events of InsP3-induced Ca2+ liberation in Xenopus oocytes: Hot spots, puffs and blips. *Cell Calcium*. **20** (2), 105–121, doi: 10.1016/S0143-4160(96)90100-1 (1996).
21. Diliberto, P. a, Wang, X.F., Herman, B. Confocal imaging of Ca2+ in cells. *Methods in Cell Biology*. **40**, 243–262, doi: 10.1016/S0091-679X(08)61117-6 (1994).
22. Martínez-Zaguilán, R., Parnami, G., Lynch, R.M. Selection of fluorescent ion indicators for simultaneous measurements of pH and Ca2+. *Cell Calcium*. **19** (4), 337–349, doi: 10.1016/S0143-4160(96)90074-3 (1996).
23. Hayashi, H., Miyata, H. Fluorescence imaging of intracellular Ca2+. *The Journal of Pharmacology & Toxicology Methods*. **31** (1), 1–10 (1994).
24. Thomas, D., Tovey, S.C., Collins, T.J., Bootman, M.D., Berridge, M.J., Lipp, P. A comparison of fluorescent Ca2+indicator properties and their use in measuring elementary and global Ca2+signals. *Cell Calcium*. **28** (4), 213–223, doi: 10.1054/ceca.2000.0152 (2000).
25. Lock, J.T., Parker, I., Smith, I.F. A comparison of fluorescent Ca2+indicators for imaging local Ca2+signals in cultured cells. *Cell Calcium*. **58** (6), 638–648, doi: 10.1016/j.ceca.2015.10.003 (2015).
26. Flagmeier, P. *et al.* Ultrasensitive Measurement of Ca 2+ Influx into Lipid Vesicles Induced by Protein Aggregates. *Angewandte Chemie International Edition*. **56** (27), 7750–7754, doi: 10.1002/anie.201700966 (2017).
27. Tsutsumi, S. *et al.* Structure-Function Relationships between Aldolase C/Zebrin II Expression and Complex Spike Synchrony in the Cerebellum. *Journal of Neuroscience*. **35** (2), 843–852, doi: 10.1523/JNEUROSCI.2170-14.2015 (2015).
28. Rietdorf, K., Chehab, T., Allman, S., Bootman, M.D. Novel improved Ca indicator dyes on the market - a comparative study of novel Ca indicators with Fluo-4. *Calcium Signalling: The Next Generation*. 590 (2014).
29. Akerboom, J. *et al.* Optimization of a GCaMP Calcium Indicator for Neural Activity Imaging. *Journal of Neuroscience*. **32** (40), 13819–13840, doi: 10.1523/JNEUROSCI.2601-12.2012 (2012).
30. Seidemann, E. *et al.* Calcium imaging with genetically encoded indicators in behaving primates. *eLife*. **5** (2016JULY), doi: 10.7554/eLife.16178 (2016).
31. Su, S. *et al.* Genetically encoded calcium indicator illuminates calcium dynamics in primary cilia. *Nature Methods*. **10** (11), 1105–1109, doi: 10.1038/nmeth.2647 (2013).

32. Kaestner, L. *et al.* Genetically encoded Ca2+ indicators in cardiac myocytes. *Circulation Research*. **114** (10), 1623–1639, doi: 10.1161/CIRCRESAHA.114.303475 (2014).
33. Tang, S., Reddish, F., Zhuo, Y., Yang, J.J. Fast kinetics of calcium signaling and sensor design. *Current Opinion in Chemical Biology*. **27**, 90–97, doi: 10.1016/j.cbpa.2015.06.014 (2015).
34. Barnett, L.M., Hughes, T.E., Drobizhev, M. Deciphering the molecular mechanism responsible for GCaMP6m's Ca2+-dependent change in fluorescence. *PLoS ONE*. **12** (2), 1–24, doi: 10.1371/journal.pone.0170934 (2017).
35. Spencer, N.J. *et al.* Identification of a rhythmic firing pattern in the enteric nervous system that generates rhythmic electrical activity in smooth muscle. *The Journal of Neuroscience*. 3489–17, doi: 10.1523/JNEUROSCI.3489-17.2018 (2018).
36. Hibberd, T.J. *et al.* Synaptic Activation of Putative Sensory Neurons By Hexamethonium-Sensitive Nerve Pathways in Mouse Colon. *American Journal of Physiology - Gastrointestinal and Liver Physiology*. (861), ajpgi.00234.2017, doi: 10.1152/ajpgi.00234.2017 (2017).
37. Baker, S.A., Drumm, B.T., Saur, D., Hennig, G.W., Ward, S.M., Sanders, K.M. Spontaneous Ca(2+) transients in interstitial cells of Cajal located within the deep muscular plexus of the murine small intestine. *The Journal of Physiology*. **594** (12), 3317–38, doi: 10.1113/JP271699 (2016).
38. Drumm, B.T. *et al.* Clustering of Ca2+ transients in interstitial cells of Cajal defines slow wave duration. *The Journal of General Physiology*. **149** (7), 703–725, doi: 10.1085/jgp.201711771 (2017).
39. Baker, S.A., Drumm, B.T., Cobine, C.A., Keef, K.D., Sanders, K.M. Inhibitory Neural Regulation of the Ca2+ Transients in Intramuscular Interstitial Cells of Cajal in the Small Intestine. *Frontiers in Physiology*. **9** (April), 1–24, doi: 10.3389/fphys.2018.00328 (2018).
40. Baker, S.A. *et al.* Excitatory Neuronal Responses of Ca 2+ Transients in Interstitial Cells of Cajal in the Small Intestine. *eNeuro*. **5** (2), ENEURO.0080-18.2018, doi: 10.1523/ENEURO.0080-18.2018 (2018).
41. Drumm, B.T., Sung, T.S., Zheng, H., Baker, S.A., Koh, S.D., Sanders, K.M. The effects of mitochondrial inhibitors on Ca2+signalling and electrical conductances required for pacemaking in interstitial cells of Cajal in the mouse small intestine. *Cell Calcium*. **72**, 1–17, doi: 10.1016/j.ceca.2018.01.003 (2018).
42. Zheng, H., Drumm, B.T., Earley, S., Sung, T.S., Koh, S.D., Sanders, K.M. SOCE mediated by STIM and Orai is essential for pacemaker activity in the interstitial cells of Cajal in the gastrointestinal tract. *Science Signaling*. **11** (June), doi: 10.1126/scisignal.aaq0918 (2018).
43. Zhu, M.H. *et al.* A Ca(2+)-activated Cl(-) conductance in interstitial cells of Cajal linked to slow wave currents and pacemaker activity. *The Journal of Physiology*. **587** (20), 4905–4918, doi: 10.1113/jphysiol.2009.176206 (2009).
44. Zhu, M.H., Sung, T.S., O'Driscoll, K., Koh, S.D., Sanders, K.M. Intracellular Ca(2+) release from endoplasmic reticulum regulates slow wave currents and pacemaker activity of interstitial cells of Cajal. *American Journal of Physiology. Cell Physiology*. **308** (8), C608-20, doi: 10.1152/ajpcell.00360.2014 (2015).
45. Zhu, M.H. *et al.* Muscarinic activation of Ca2+-activated Cl- current in interstitial cells of Cajal. *The Journal of Physiology*. **589** (Pt 18), 4565–4582, doi: 10.1113/jphysiol.2011.211094 (2011).

46. Ward, S.M., Burns, A.J., Torihashi, S., Sanders, K.M. Mutation of the proto-oncogene c-kit blocks development of interstitial cells and electrical rhythmicity in murine intestine. *The Journal of Physiology*. **480** (Pt 1), 91–97, doi: 10.1113/jphysiol.1994.sp020343 (1994).
47. Huizinga, J.D., Thuneberg, L., Klüppel, M., Malysz, J., Mikkelsen, H.B., Bernstein, A. W/kit gene required for interstitial cells of cajal and for intestinal pacemaker activity. *Nature*. **373** (6512), 347–349, doi: 10.1038/373347a0 (1995).
48. Ordog, T., Ward, S.M., Sanders, K.M. Interstitial cells of Cajal generate electricial slow waves in the murine stomach. *The Journal of Physiology*. **518** (1), 257–269 (1999).
49. Sanders, K.M., Ward, S.M., Koh, S.D. Interstitial cells: regulators of smooth muscle function. *Physiological Reviews*. **94** (3), 859–907, doi: 10.1152/physrev.00037.2013 (2014).
50. Ward, S.M., McLaren, G.J., Sanders, K.M. Interstitial cells of Cajal in the deep muscular plexus mediate enteric motor neurotransmission in the mouse small intestine. *The Journal of Physiology*. **573** (1), 147–159, doi: 10.1113/jphysiol.2006.105189 (2006).
51. Komuro, T. Structure and organization of interstitial cells of Cajal in the gastrointestinal tract. *The Journal of Physiology*. **576** (3), 653–658, doi: 10.1113/jphysiol.2006.116624 (2006).
52. Komuro, T. Comparative morphology of interstitial cells of Cajal: ultrastructural characterization. *Microscopy Research and Technique*. **47** (4), 267–285, doi: 10.1002/(SICI)1097-0029(19991115)47:4<267::AID-JEMT5>3.0.CO;2-O (1999).
53. Sanders, K.M., Ward, S.M., Koh, S.D. Interstitial Cells: Regulators of Smooth Muscle Function. *Physiological Reviews*. **94** (3), 859–907, doi: 10.1152/physrev.00037.2013 (2014).
54. Ye, L., Haroon, M.A., Salinas, A., Paukert, M. Comparison of GCaMP3 and GCaMP6f for studying astrocyte Ca2+dynamics in the awake mouse brain. *PLoS ONE*. **12** (7), e0181113, doi: 10.1371/journal.pone.0181113 (2017).
55. Truett, G.E., Heeger, P., Mynatt, R., Truett, A.A., Walker, J.A., Warman, M.L. Preparation of PCR quality mouse genomic DNA with hot sodium hydroxide and Tris (HotSHOT). *BioTechniques.* **29** (52), 54, doi: 10.2144/00291bm09 (2000).
56. The Jackson Laboratory. <https://www2.jax.org/protocolsdb/f?p=116:5:0::NO:5:P5_MASTER_PROTOCOL_ID,P5_JRS_CODE:27076,028865> (2017).
57. Drumm, B.T. *et al.* Ca 2+ signalling in mouse urethral smooth muscle *in situ* : role of Ca 2+ stores and Ca 2+ influx mechanisms. *The Journal of Physiology*. **596** (8), 1433–1466, doi: 10.1113/JP275719 (2018).
58. Heppner, T.J., Hennig, G.W., Nelson, M.T., Vizzard, M.A. Rhythmic Calcium Events in the Lamina Propria Network of the Urinary Bladder of Rat Pups. *Frontiers in Systems Neuroscience*. **11** (December), 1–16, doi: 10.3389/fnsys.2017.00087 (2017).
59. Heppner, T.J., Hennig, G.W., Nelson, M.T., May, V., Vizzard, M.A. PACAP38-Mediated Bladder Afferent Nerve Activity Hyperexcitability and Ca 2 + Activity in Urothelial Cells from Mice. *Journal of Molecular Neuroscience*. **1** (2018).
60. Griffin, C.S. *et al.* Muscarinic Receptor Induced Contractions of the Detrusor are Mediated by Activation of TRPC4 Channels. *Journal of Urology*. **196** (6), 1796–1808, doi: 10.1016/j.juro.2016.05.108 (2016).
61. Sergeant, G.P., Craven, M., Hollywood, M.A., Mchale, N.G., Thornbury, K.D. Spontaneous

Ca2+waves in rabbit corpus cavernosum: Modulation by nitric oxide and cGMP. *Journal of Sexual Medicine*. **6** (4), 958–966, doi: 10.1111/j.1743-6109.2008.01090.x (2009).

62. Bradley, E. *et al.* Novel Excitatory Effects of Adenosine Triphosphate on Contractile and Pacemaker Activity in Rabbit Urethral Smooth Muscle. *Journal of Urology*. **183** (2), 801–811, doi: 10.1016/j.juro.2009.09.075 (2010).
63. Drumm, B.T. *et al.* The effect of high [K +] o on spontaneous Ca 2+ waves in freshly isolated interstitial cells of Cajal from the rabbit urethra. *Physiological Reports*. **2** (1), e00203, doi: 10.1002/phy2.203 (2014).

Figure

Click here to access/download;Figure;Figure 1.pdf

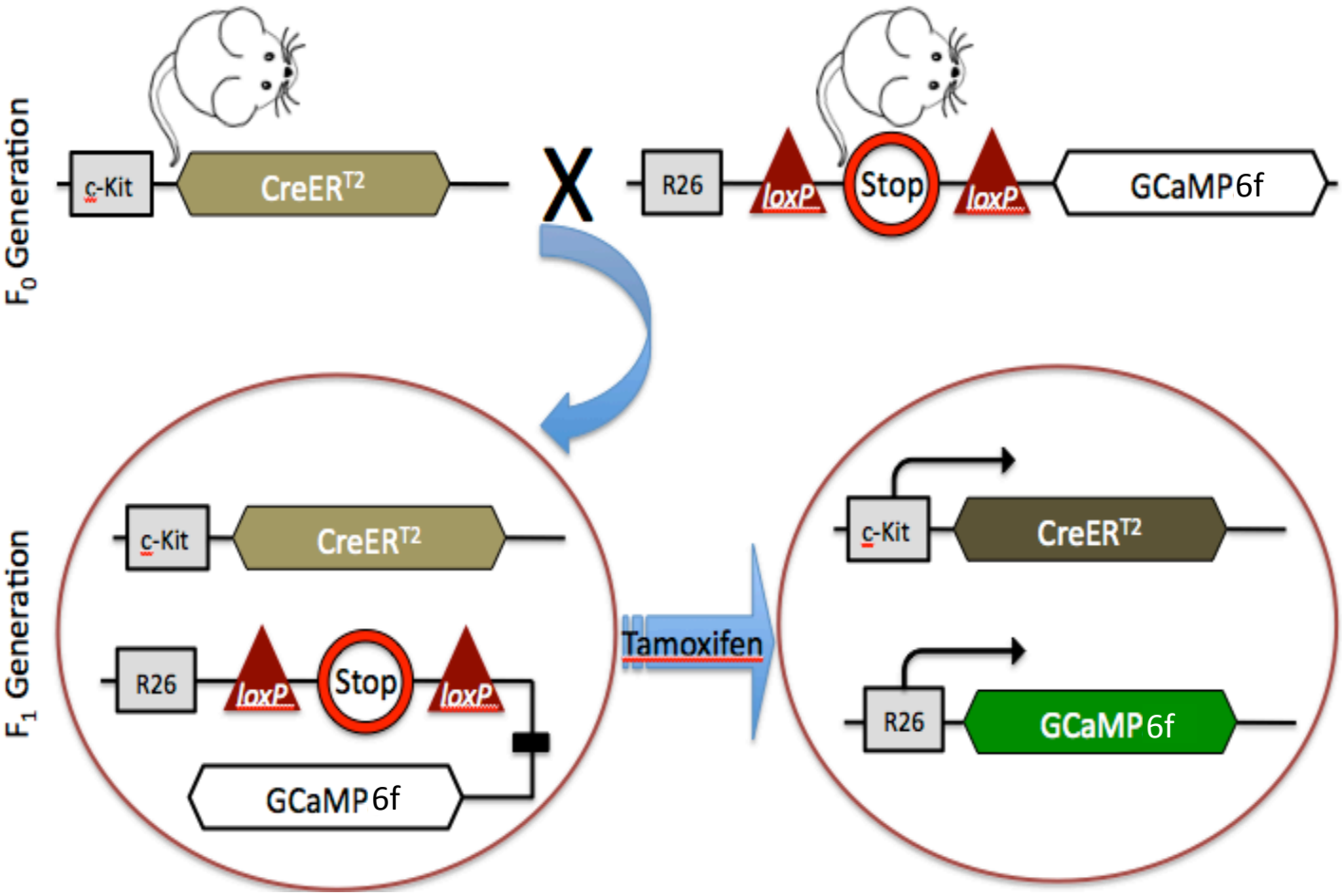

Figure

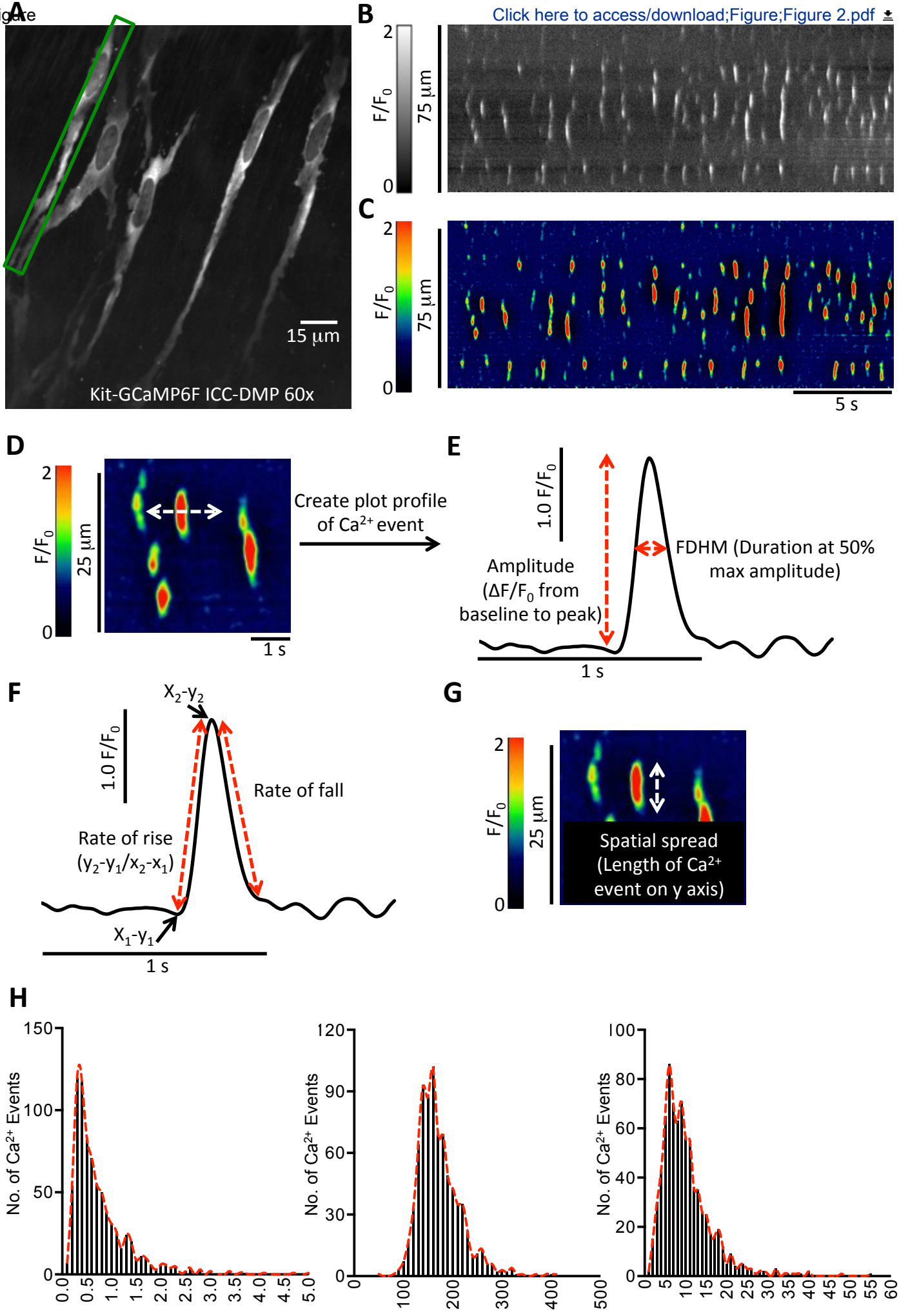

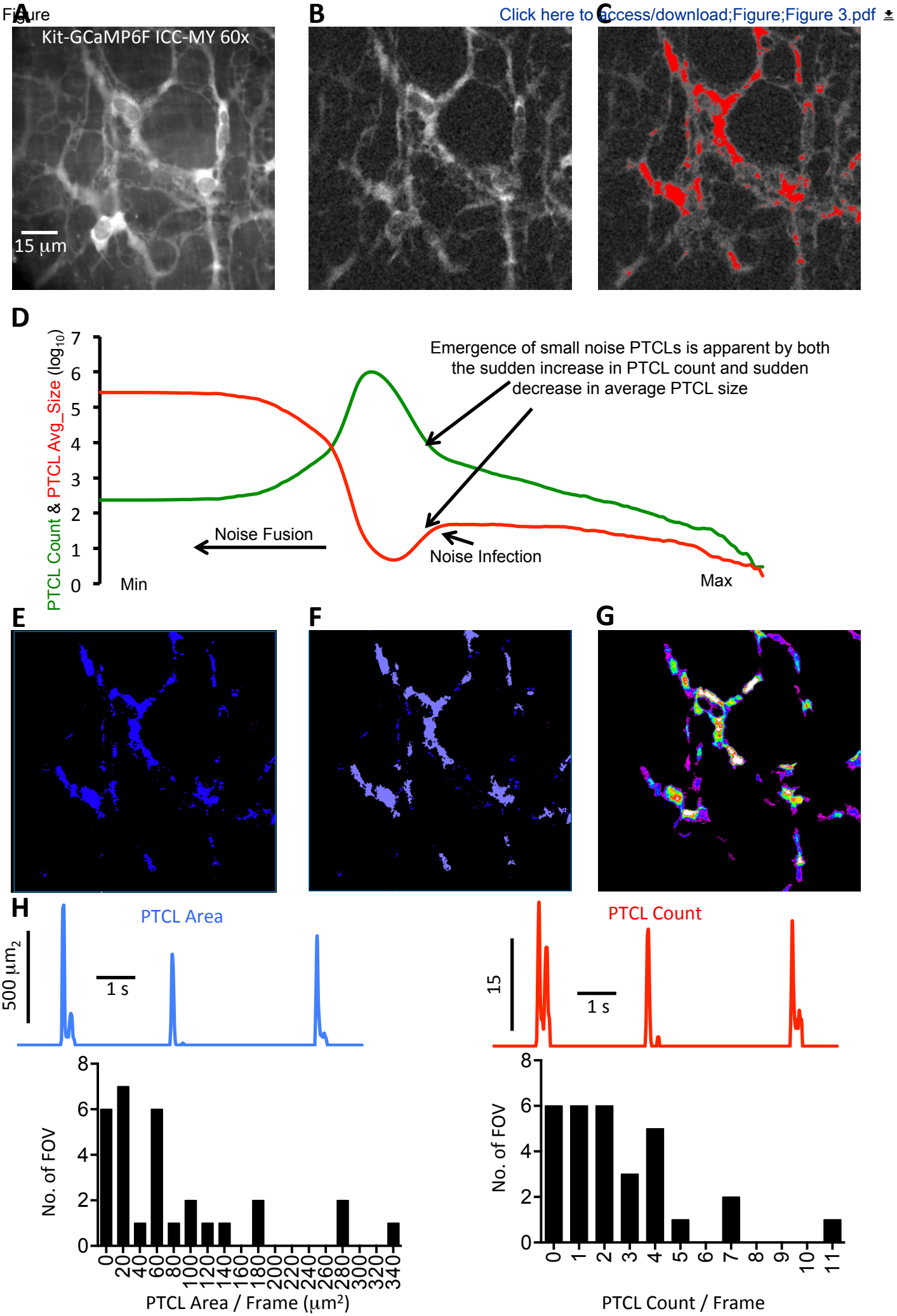

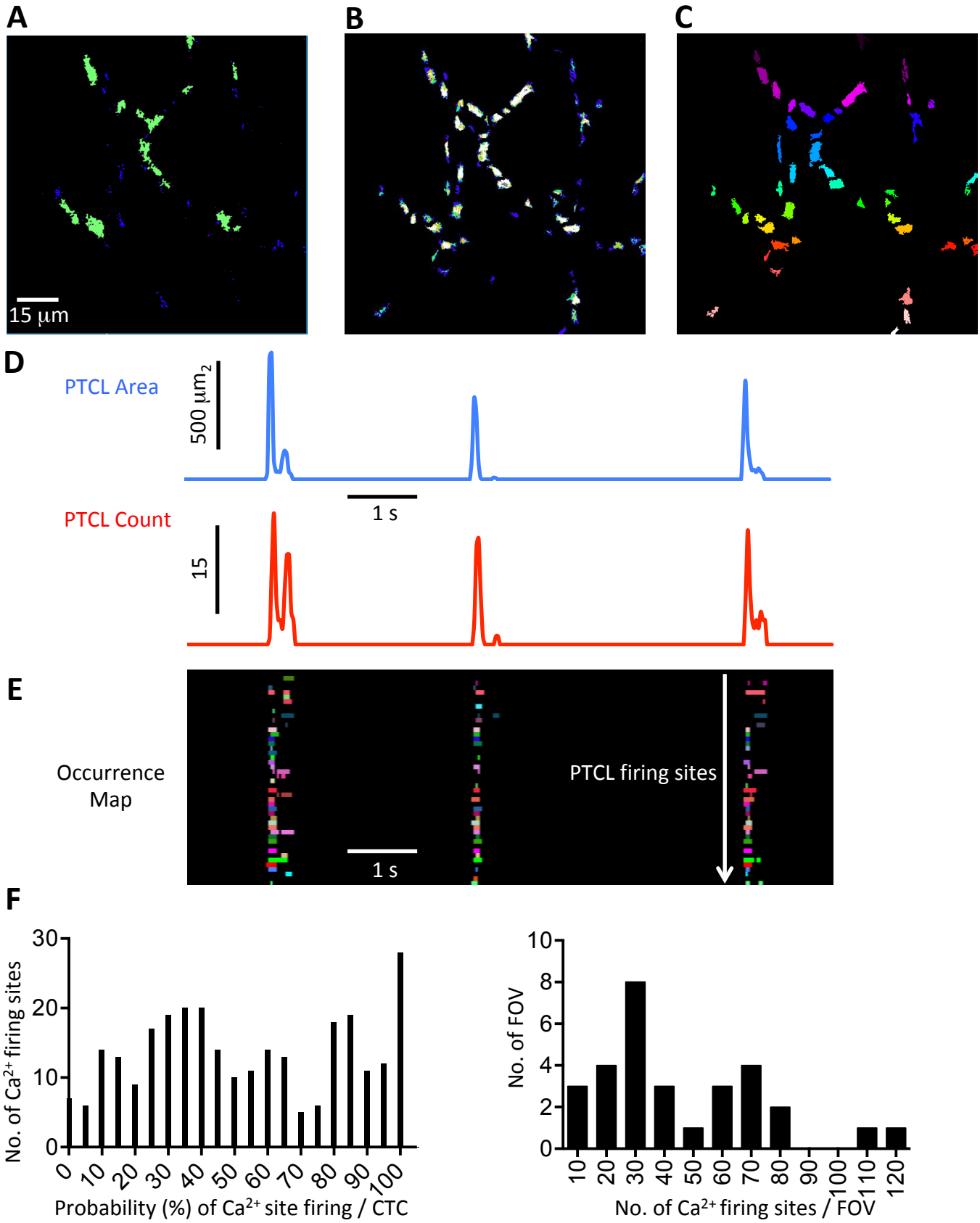

Table of Materials

Click here to access/download;Table of Materials;JoVE_Materials Revised.xlsx

Name of Material/ Equipment	Company
Image J software	NIH
Volumetry	GWH
Isoflurane	Baxter, Deerfield, IL, l
Tamoxifen	Sigma
GCaMP6F mice	Jackson Laboratory
Kit-Cre mice	Gifted From Dr. Diete
Ethanol	Pharmco-Aaper

Catalog Number	Comments/Description
1.5a	Image J software
Volumetry 8Gd	Custom made analysis software
NDC 10019-360-60	
T5648	
Ai95 (RCL-GCaMP6f)-D	
c-Kit$^{+/Cre-ERT2}$	
SDA 2B-6	

1 Alewife Center #200
Cambridge, MA 02140
tel. 617.945.9051
www.jove.com

ARTICLE AND VIDEO LICENSE AGREEMENT

Title of Article:	Applications of spatio-temporal mapping and particle analysis techniques to quantify intracellular Ca2+ signaling in situ
Author(s):	Bernard T. Drumm, Grant W. Hennig, Salah A. Baker & Kenton M. Sanders.

Item 1: The Author elects to have the Materials be made available (as described at http://www.jove.com/publish) via:

☒ Standard Access ☐ Open Access

Item 2: Please select one of the following items:

☒ The Author is **NOT** a United States government employee.

☐ The Author is a United States government employee and the Materials were prepared in the course of his or her duties as a United States government employee.

☐ The Author is a United States government employee but the Materials were NOT prepared in the course of his or her duties as a United States government employee.

ARTICLE AND VIDEO LICENSE AGREEMENT

1. **Defined Terms.** As used in this Article and Video License Agreement, the following terms shall have the following meanings: "**Agreement**" means this Article and Video License Agreement; "**Article**" means the article specified on the last page of this Agreement, including any associated materials such as texts, figures, tables, artwork, abstracts, or summaries contained therein; "**Author**" means the author who is a signatory to this Agreement; "**Collective Work**" means a work, such as a periodical issue, anthology or encyclopedia, in which the Materials in their entirety in unmodified form, along with a number of other contributions, constituting separate and independent works in themselves, are assembled into a collective whole; "**CRC License**" means the Creative Commons Attribution-Non Commercial-No Derivs 3.0 Unported Agreement, the terms and conditions of which can be found at: http://creativecommons.org/licenses/by-nc-nd/3.0/legalcode; "**Derivative Work**" means a work based upon the Materials or upon the Materials and other pre-existing works, such as a translation, musical arrangement, dramatization, fictionalization, motion picture version, sound recording, art reproduction, abridgment, condensation, or any other form in which the Materials may be recast, transformed, or adapted; "**Institution**" means the institution, listed on the last page of this Agreement, by which the Author was employed at the time of the creation of the Materials; "**JoVE**" means MyJove Corporation, a Massachusetts corporation and the publisher of The Journal of Visualized Experiments; "**Materials**" means the Article and / or the Video; "**Parties**" means the Author and JoVE; "**Video**" means any video(s) made by the Author, alone or in conjunction with any other parties, or by JoVE or its affiliates or agents, individually or in collaboration with the Author or any other parties, incorporating all or any portion of the Article, and in which the Author may or may not appear.

2. **Background.** The Author, who is the author of the Article, in order to ensure the dissemination and protection of the Article, desires to have the JoVE publish the Article and create and transmit videos based on the Article. In furtherance of such goals, the Parties desire to memorialize in this Agreement the respective rights of each Party in and to the Article and the Video.

3. **Grant of Rights in Article.** In consideration of JoVE agreeing to publish the Article, the Author hereby grants to JoVE, subject to **Sections 4** and **7** below, the exclusive, royalty-free, perpetual (for the full term of copyright in the Article, including any extensions thereto) license (a) to publish, reproduce, distribute, display and store the Article in all forms, formats and media whether now known or hereafter developed (including without limitation in print, digital and electronic form) throughout the world, (b) to translate the Article into other languages, create adaptations, summaries or extracts of the Article or other Derivative Works (including, without limitation, the Video) or Collective Works based on all or any portion of the Article and exercise all of the rights set forth in (a) above in such translations, adaptations, summaries, extracts, Derivative Works or Collective Works and(c) to license others to do any or all of the above. The foregoing rights may be exercised in all media and formats, whether now known or hereafter devised, and include the right to make such modifications as are technically necessary to exercise the rights in other media and formats. If the "Open Access" box has been checked in **Item 1** above, JoVE and the Author hereby grant to the public all such rights in the Article as provided in, but subject to all limitations and requirements set forth in, the CRC License.

4. **Retention of Rights in Article.** Notwithstanding the exclusive license granted to JoVE in **Section 3** above, the Author shall, with respect to the Article, retain the non-exclusive right to use all or part of the Article for the non-commercial purpose of giving lectures, presentations or teaching classes, and to post a copy of the Article on the Institution's website or the Author's personal website, in each case provided that a link to the Article on the JoVE website is provided and notice of JoVE's copyright in the Article is included. All non-copyright intellectual property rights in and to the Article, such as patent rights, shall remain with the Author.

5. **Grant of Rights in Video – Standard Access.** This **Section 5** applies if the "Standard Access" box has been checked in **Item 1** above or if no box has been checked in **Item 1** above. In consideration of JoVE agreeing to produce, display or otherwise assist with the Video, the Author hereby acknowledges and agrees that, Subject to **Section 7** below, JoVE is and shall be the sole and exclusive owner of all rights of any nature, including, without limitation, all copyrights, in and to the Video. To the extent that, by law, the Author is deemed, now or at any time in the future, to have any rights of any nature in or to the Video, the Author hereby disclaims all such rights and transfers all such rights to JoVE.

6. **Grant of Rights in Video – Open Access.** This **Section 6** applies only if the "Open Access" box has been checked in **Item 1** above. In consideration of JoVE agreeing to produce, display or otherwise assist with the Video, the Author hereby grants to JoVE, subject to **Section 7** below, the exclusive, royalty-free, perpetual (for the full term of copyright in the Article, including any extensions thereto) license (a) to publish, reproduce, distribute, display and store the Video in all forms, formats and media whether now known or hereafter developed (including without limitation in print, digital and electronic form) throughout the world, (b) to translate the Video into other languages, create adaptations, summaries or extracts of the Video or other Derivative Works or Collective Works based on all or any portion of the Video and exercise all of the rights set forth in (a) above in such translations, adaptations, summaries, extracts, Derivative Works or Collective Works and (c) to license others to do any or all of the above. The foregoing rights may be exercised in all media and formats, whether now known or hereafter devised, and include the right to make such modifications as are technically necessary to exercise the rights in other media and formats. For any Video to which this **Section 6** is applicable, JoVE and the Author hereby grant to the public all such rights in the Video as provided in, but subject to all limitations and requirements set forth in, the CRC License.

7. **Government Employees.** If the Author is a United States government employee and the Article was prepared in the course of his or her duties as a United States government employee, as indicated in **Item 2** above, and any of the licenses or grants granted by the Author hereunder exceed the scope of the 17 U.S.C. 403, then the rights granted hereunder shall be limited to the maximum rights permitted under such statute. In such case, all provisions contained herein that are not in conflict with such statute shall remain in full force and effect, and all provisions contained herein that do so conflict shall be deemed to be amended so as to provide to JoVE the maximum rights permissible within such statute.

8. **Protection of the Work.** The Author(s) authorize JoVE to take steps in the Author(s) name and on their behalf if JoVE believes some third party could be infringing or might infringe the copyright of either the Author's Article and/or Video.

9. **Likeness, Privacy, Personality.** The Author hereby grants JoVE the right to use the Author's name, voice, likeness, picture, photograph, image, biography and performance in any way, commercial or otherwise, in connection with the Materials and the sale, promotion and distribution thereof. The Author hereby waives any and all rights he or she may have, relating to his or her appearance in the Video or otherwise relating to the Materials, under all applicable privacy, likeness, personality or similar laws.

10. **Author Warranties.** The Author represents and warrants that the Article is original, that it has not been published, that the copyright interest is owned by the Author (or, if more than one author is listed at the beginning of this Agreement, by such authors collectively) and has not been assigned, licensed, or otherwise transferred to any other party. The Author represents and warrants that the author(s) listed at the top of this Agreement are the only authors of the Materials. If more than one author is listed at the top of this Agreement and if any such author has not entered into a separate Article and Video License Agreement with JoVE relating to the Materials, the Author represents and warrants that the Author has been authorized by each of the other such authors to execute this Agreement on his or her behalf and to bind him or her with respect to the terms of this Agreement as if each of them had been a party hereto as an Author. The Author warrants that the use, reproduction, distribution, public or private performance or display, and/or modification of all or any portion of the Materials does not and will not violate, infringe and/or misappropriate the patent, trademark, intellectual property or other rights of any third party. The Author represents and warrants that it has and will continue to comply with all government, institutional and other regulations, including, without limitation all institutional, laboratory, hospital, ethical, human and animal treatment, privacy, and all other rules, regulations, laws, procedures or guidelines, applicable to the Materials, and that all research involving human and animal subjects has been approved by the Author's relevant institutional review board.

11. **JoVE Discretion.** If the Author requests the assistance of JoVE in producing the Video in the Author's facility, the Author shall ensure that the presence of JoVE employees, agents or independent contractors is in accordance with the relevant regulations of the Author's institution. If more than one author is listed at the beginning of this Agreement, JoVE may, in its sole

jove JOURNAL OF VISUALIZED EXPERIMENTS
1 Alewife Center #200
Cambridge, MA 02140
tel. 617.945.9051
www.jove.com

ARTICLE AND VIDEO LICENSE AGREEMENT

discretion, elect not take any action with respect to the Article until such time as it has received complete, executed Article and Video License Agreements from each such author. JoVE reserves the right, in its absolute and sole discretion and without giving any reason therefore, to accept or decline any work submitted to JoVE. JoVE and its employees, agents and independent contractors shall have full, unfettered access to the facilities of the Author or of the Author's institution as necessary to make the Video, whether actually published or not. JoVE has sole discretion as to the method of making and publishing the Materials, including, without limitation, to all decisions regarding editing, lighting, filming, timing of publication, if any, length, quality, content and the like.

12. **Indemnification.** The Author agrees to indemnify JoVE and/or its successors and assigns from and against any and all claims, costs, and expenses, including attorney's fees, arising out of any breach of any warranty or other representations contained herein. The Author further agrees to indemnify and hold harmless JoVE from and against any and all claims, costs, and expenses, including attorney's fees, resulting from the breach by the Author of any representation or warranty contained herein or from allegations or instances of violation of intellectual property rights, damage to the Author's or the Author's institution's facilities, fraud, libel, defamation, research, equipment, experiments, property damage, personal injury, violations of institutional, laboratory, hospital, ethical, human and animal treatment, privacy or other rules, regulations, laws, procedures or guidelines, liabilities and other losses or damages related in any way to the submission of work to JoVE, making of videos by JoVE, or publication in JoVE or elsewhere by JoVE. The Author shall be responsible for, and shall hold JoVE harmless from, damages caused by lack of sterilization, lack of cleanliness or by contamination due to the making of a video by JoVE its employees, agents or independent contractors. All sterilization, cleanliness or decontamination procedures shall be solely the responsibility of the Author and shall be undertaken at the Author's expense. All indemnifications provided herein shall include JoVE's attorney's fees and costs related to said losses or damages. Such indemnification and holding harmless shall include such losses or damages incurred by, or in connection with, acts or omissions of JoVE, its employees, agents or independent contractors.

13. **Fees.** To cover the cost incurred for publication, JoVE must receive payment before production and publication the Materials. Payment is due in 21 days of invoice. Should the Materials not be published due to an editorial or production decision, these funds will be returned to the Author. Withdrawal by the Author of any submitted Materials after final peer review approval will result in a US$1,200 fee to cover pre-production expenses incurred by JoVE. If payment is not received by the completion of filming, production and publication of the Materials will be suspended until payment is received.

14. **Transfer, Governing Law.** This Agreement may be assigned by JoVE and shall inure to the benefits of any of JoVE's successors and assignees. This Agreement shall be governed and construed by the internal laws of the Commonwealth of Massachusetts without giving effect to any conflict of law provision thereunder. This Agreement may be executed in counterparts, each of which shall be deemed an original, but all of which together shall be deemed to me one and the same agreement. A signed copy of this Agreement delivered by facsimile, e-mail or other means of electronic transmission shall be deemed to have the same legal effect as delivery of an original signed copy of this Agreement.

A signed copy of this document must be sent with all new submissions. Only one Agreement is required per submission.

CORRESPONDING AUTHOR

Name:	Bernard T. Drumm
Department:	Physiology & Cell Biology
Institution:	University of Nevada, Reno School of Medicine
Title:	Dr.
Signature:	Bernard Drumm Digitally signed by Bernard Drumm DN: cn=Bernard Drumm, o, ou, email=bdrumm@unr.edu, c=US Date: 2018.08.23 16:20:03 -08'00'
Date:	August 23rd 2018

Please submit a **signed** and **dated** copy of this license by one of the following three methods:

1. Upload an electronic version on the JoVE submission site
2. Fax the document to +1.866.381.2236
3. Mail the document to JoVE / Attn: JoVE Editorial / 1 Alewife Center #200 / Cambridge, MA 02140

Editorial comments:

Changes to be made by the author(s) regarding the written manuscript:

1. Please take this opportunity to thoroughly proofread the manuscript to ensure that there are no spelling or grammar issues.

We have proofread the manuscript for spelling and grammar issues.

2. Please revise lines 504-505 to avoid previously published text.

These lines have been revised.

3. Please provide an email address for each author.

The email address for each author is now listed on the title page.

4. JoVE cannot publish manuscripts containing commercial language. This includes trademark symbols (™), registered symbols (®), and company names before an instrument or reagent. Please remove all commercial language from your manuscript and use generic terms instead. All commercial products should be sufficiently referenced in the Table of Materials and Reagents. You may use the generic term followed by "(see table of materials)" to draw the readers' attention to specific commercial names. Examples of commercial sounding language in your manuscript are: Jackson Laboratory, Sigma, Pharmco-Aaper, Baxter, etc.

We have removed commercial names from the manuscript and updated the table of materials and reagents accordingly.

5. Please revise the protocol text to avoid the use of any personal pronouns (e.g., "we", "you", "our" etc.).

We have revised the manuscript to avoid the use of personal pronouns.

6. Please revise the protocol to contain only action items that direct the reader to do something (e.g., "Do this," "Ensure that," etc.). The actions should be described in the imperative tense in complete sentences wherever possible. Avoid usage of phrases such as "could be," "should be," and "would be" throughout the Protocol. Any text that cannot be written in the imperative tense may be added as a "Note." Please include all safety procedures and use of hoods, etc. However, notes should be used sparingly and actions should be described in the imperative tense wherever possible.

We have revised the manuscript and used the imperative tense whenever possible.

7. 1.5: Please describe how to confirm GCaMP6f expression by genotyping or add a relevant reference.

We have added the detail of how GCaMP6f was confirmed with genotyping in the revised manuscript.

8. 2.1: Please specify the concentration of isoflurane.

The concentration of isoflurane used is now included in the revised manuscript.

9. 2.2: Please provide the composition of Krebs-Ringer bicarbonate solution. If it is purchased, please cite the Table of Materials.

The KRB solution composition is now inserted into the revised manuscript.

10. 2.5, 3.1, 3.18, 3.19, 4.1, etc.: The Protocol should be made up almost entirely of discrete steps without large paragraphs of text between sections. Please simplify the Protocol so that individual steps contain only 2-3 actions per step and a maximum of 4 sentences per step. Use sub-steps as necessary. Please move the discussion about the protocol to the Discussion.

We have revised and simplified the protocol and ensured that the protocol steps are shorter throughout.

11. After you have made all the recommended changes to your protocol (listed above), please highlight 2.75 pages or less of the Protocol (including headings and spacing) that identifies the essential steps of the protocol for the video, i.e., the steps that should be visualized to tell the most cohesive story of the Protocol.

The text deemed most appropriate has been highlighted.

12. Please highlight complete sentences (not parts of sentences). Please ensure that the highlighted part of the step includes at least one action that is written in imperative tense. Please do not highlight any steps describing anesthetization and euthanasia.

The text deemed most appropriate has been highlighted.

13. Please include all relevant details that are required to perform the step in the highlighting. For example: If step 2.5 is highlighted for filming and the details of how to perform the step are given in steps 2.5.1 and 2.5.2, then the sub-steps where the details are provided must be highlighted.

The text deemed most appropriate has been highlighted.

14. Please upload each Figure individually to your Editorial Manager account as a .png, .tiff, .pdf, .svg, .eps, .psd, or .ai file.

Figures have been uploaded as requested.

15. Figure 2H: The x-axis in the middle panel is cut off. Please fix it.

This has been corrected.

16. Discussion: Please also discuss any limitations of the technique.

Limitations of the technique are now discussed.

17. References: Please do not abbreviate journal titles.

Journal titles are not abbreviated.

18. Please revise the table of the essential supplies, reagents, and equipment to include the name, company, and catalog number of all relevant materials.

Now revised.

Reviewers' comments:

Reviewer #1:

Manuscript Summary:
The authors have a rich publication history utilizing elegant calcium imaging preparations with a rigorous analysis focused on providing quantitative parameters to describe the observed phenomena. The manuscript titled "Applications of spatio-temporal mapping and particle analysis techniques to quantify intracellular Ca2+ signaling in situ" primarily provides a step by step protocol detailing their Ca2+ acquisition process and Ca2+ video analysis protocol that can be readily applied to other tissues in addition to the intestinal ICC imaging described here. The generation of ICC targeted GCaMP6f expression using the Cre-Lox system under control of a tamoxifen inducible cKit-Cre is described, and followed by the method of preparation and Ca2+ imaging of the intestinal ICCs. The authors then describe an improved ROI method for analyzing Ca2+ videos using spatio-temporal maps to allow for quantification of Ca2+ events beyond simple intensity-time plots including production of informative STM plots, F/F0 values, spatial spread and velocity of Ca2+ events, and rise/decay/total time of events. The authors then describe a step by step procedure using a custom software Volumetry to analyze an entire FOV of a complex Ca2+ recording in an unbiased and efficient manner. Some explanation of the power and limitations of the protocols described here are discussed and evidence given for their practical applications in other tissue beds.

Minor Concerns:
The protocols are written in a clear and succinct manner. The STM protocol outlined in section 3 was easily followed by this reviewer using ImageJ and the described results from Figure 2 were readily achieved using Ca2+ recordings from non-ICC cells. However, the bias inherent to the user generated ROI is still a potential downfall. The STM created from the rectangle ROI used in Volumetry appears to be an average value of (STMAvgRow) the intensity across either the y or x axis, and I am curious if signal amplitude could be inadvertently diluted if the Ca2+ is highly localized and substantially smaller than the width of the ROI.

The reviewer is correct in this observation. We have added a statement in the discussion regarding the potential dilution of the calcium signal amplitude if the width of the ROI is drawn too wide.

Tangentially, taking intensity measurements from a single line through the midpoint axis of a cell as described in section 3.12 is also subject to the proximity of the Ca2+ event to the user generated line for the STM. This may be easily disregarded in spindle like longitudinal cells such as the ICC-DMP as the authors point out in Section 4.1, but may be worth adding a few sentences in the discussion for awareness to these potential issues in the broader application of this method.

As the reviewer suggests, we have added additional information in the discussion highlighting these key areas of analysis consideration.

The PTCL analysis using Volumetry is especially powerful in its ability to analyze an entire field of view in an unbiased manner. Widespread use of the protocols listed will likely depend on the means and ease of availability and acquisition of the Volumetry program. For section 4.3 and 4.4 the reader is told to run the STK Filter Differentiate and a STK Filter-Gauss KRNL, and are told that a value of 2 and 5 work well respectively. It may be helpful to provide what the reasonable range for the values one should expect to use to prevent or the conditions that would lead to changing those values from what is suggested.

As the reviewer suggests, we have added additional information in the discussion describing more details about the range of differentiation values to be applied across different recordings and also the consequences on noise and signal to noise ratios of applying too low or too high a differentiation value. We added the following statement to further clarify the role of the differentiation function. We have added the following statement to the manuscript to further clarify the differentiation function in Volumetry. "*Note: Differentiation in this context will reduce the intensity of areas of recording (pixels) that show no dynamic activity over the number of frames specified. Thus, if a value of '2' is inserted, each pixel in every frame of the recording is analysed and if within that frame there is no dynamic change in pixel fluorescence 1 frame before and 1 frame after, the intensity within those pixels will be subtracted*

from the recording. Thus non-dynamic background noise is removed and signal to noise is increased."

In the section utilizing Image J, I would suggest to mention or consider adding the plot profile command in section 3.7 and 3.17 to provide a visual image of the calcium intensity trace, whereupon the background or baseline intensity value taken from the histogram can be simply and quickly confirmed visually across time (information lost in the histogram) prior to subtraction and normalization.

We would not recommend using the plot profile command at this juncture of the protocol as the plot command profile does not give an accurate representation of intensity against time for stacked TIFF images in ImageJ. While the command for plot profile generates very accurate plots of fluorescence taken from single TIFF images such as the STMs described, in order to gain accurate plot profiles from the movie itself, further calibrations for space and time would need to be inserted into the raw movie, which would serve to lengthen and complicate the analysis protocol.

Line 282 Would using the median or mode, as opposed to the mean, be less sensitive to potential outlier signal events within the background ROI (or incidental inclusion of the targeted cell population). Introduction of outlier signal noise within this background ROI could inadvertently result in some signal loss.

In our experience, the use of the mean value for subtraction purposes yields the most consistent normalization for movie recordings. While as the reviewer suggests, the use of the mode or median can be beneficial in certain recordings, in order to consistently apply the same analysis to all recordings the mean is the most consistent representation of background noise (at least for our recordings).

Minor Edits:
Line 141/2: For consistency with the rest of manuscript stick with "seconds"

Edited.

Line 181: Assume Safflower "Oil"

Correct, now edited.

Line 404: "wave speed plugin" should be cited or in the very least provide the website address to access the plugin mentioned.

Upon searching for the appropriate plugin online to provide a link, it appears that this plugin is now longer available for public download and thus all reference to its implication has been removed from the manuscript.

Line 556 I assume should read Fig 4D-E.

Correct, now edited.

Reviewer #2:

Manuscript Summary:
This article describes the uses of Cre-Lox recombination to genetically insert a calcium indicator into a specific cell type - known as the Interstitial Cell of Cajal (ICC). Then, the study describes how to analyze calcium transients within ICC. While cre-lox recombination is not new, nor is the use of genetically encoded calcium indicators, the analysis approaches are useful. The methods of analysis appear to have been used previously in the Baker S et al. J. Physiol. paper, but this JOVE article explains in more detail how to use Volumetry. The analytical methods in this paper could be useful to the field, not just ICC. In fact, as there are increasingly few laboratories imaging ICC (I don't know any other laboratories doing imaging of ICC anymore, my feeling is the analysis methodology in this paper would more likely be useful to others using imaging in other cell types e.g. central neurons or brain slices. There are some bold statements that need to be reworded and supported by references. There are also some additional new references that need to be inserted, before any further editorial consideration can be given. The figures are clear and references suitable - when modified.

Major Concerns:
Line 84: it is stated "While newer Ca2+ indicator dyes such as Cal520/590 have improved the photobleaching difficulties associated with older dyes somewhat, it still remains a concern for investigators." Do the authors have a reference to support this statement ? Reference 24 (Thomas et al. (2000) Cell Calcium) does not show that new calcium indicators have less photobleaching than older indicators as it was published in 2000, and the new indicators were not around then. Please explain what data this comments is based on.

We have now added new references that point out photo-bleaching effects of the Cal lines of calcium indicator dyes (Flagmeier et al., 2017; Tsutsumi et al., 2015; Rietdorf et al., 2014), highlighting that photobleaching still occurs with preparations loaded with Cal 520 and in a quantitative study was found to have similar photobleaching effects as Fluo 4.

Whilst genetically encoding calcium indicators have some clear benefits they do involve genetically modifying the animal. To provide a balanced view, the authors need to acknowledge that an important benefit of not using genetically-modified animals is the animals do not have to be genetically modified. In the introduction please insert:
"Whilst genetically-encoded calcium indicators can offer some clear advantages, recent studies have revealed that calcium imaging can be successfully performed from large populations of different neurochemical classes of neurons simultaneously using conventional calcium indicators that are not genetically encoded into the animal (Spencer NJ et al. 2018; J. Neuroci). This approach used

post-hoc immunohistochemistry to reveal multiple different classes of neurons firing at high frequency in synchronized bursts, and avoided the potential that genetic modifications to the animal may have interfered with the physiological behaviour the investigator seeks to understand (Spencer NJ et al. 2018; J. Neuroci; Hibberd T et al. AJP, 2018).

We have inserted the requested statement and the appropriate references.

Line 83: It is stated "While newer Ca2+ indicator dyes such as Cal520/590 have improved the photobleaching difficulties associated with older dyes somewhat, it still remains a concern for investigators." Do the authors have a reference to support this statement ? That is, has anyone published that newer calcium indicators confer less photo-bleaching than older indicators, or is this a subjective view ? If the author's don't have a reference to support this statement, then please reword this to state that this comment reflects the authors personal view (if that is indeed what they believe).

As stated above, we have provided new references to appropriately account for our statement in this paragraph.

Line 111: Again, it is stated "Another advantage of GECIs over traditional Ca2+ indicators is that photobleaching is reduced, as compared to dye-loaded specimens, particularly at high magnification and high rates of image capture." Again, is there a study that has systematically quantified this and published it ? If so, please include the reference. If not, reword the statement to say this is purely the authors views (again, if they believe this to be true). Otherwise, without any reference, the statement is ill-founded.

We have added an appropriate reference to the manuscript to substantiate our statement here. We draw particular attention to the paragraph in the cited paper (Barnett et al., 2017)*"The remarkable redistribution of the GCaMP chromophore from neutral to anionic forms has two important consequences. First, with 470 nm excitation, the Ca^{2+} sensor is dark at low Ca^{2+} concentrations, and only fluorescent in active cells, producing an excellent signal-to-noise ratio in complex tissues like the brain. Second, since the neutral form of the chromophore is not absorbing the 470 nm light, the Ca^{2+} sensor is only susceptible to bleaching during the brief periods that the cell is active."*

The methodology provided to run Volumetry appears to be written clearly and should be able to be followed by others.

References that need to be inserted
Hibberd T et al. (2018) AJP; https://www.ncbi.nlm.nih.gov/pubmed/28935683
Spencer NJ et al. (2018) J. Neurosci:
https://www.ncbi.nlm.nih.gov/pubmed/29807910

We have added the requested references.

Minor Concerns:
In the abstract: Change the words "the biological information" to "some biological information".

Edited as requested.

Reviewer #3:
Manuscript Summary:
Overall, the method seems to be a worthwhile one and worthy of publication in JOVE. A useful description of the experimental method used to acquire the Ca signals is presented and I see no particular problems with that.
The analysis workflow for the STM and particle analysis is presented in a very basic step by step fashion which would benefit in some places with a clearer explanation of the processing function taking place at that point.

Major Concerns:
316 Normally, the signal to noise of the created linescan will need to be improved. Do this by
317 clicking 'Auto' on the B&C HUD.

This procedure simply adjusts the image contrast to make the linescan image optimally visible to the viewer. It does not improve signal-noise and should not be referred to as doing so.

The reviewer is indeed correct here. We have edited this statement to say that the contrast and not signal to noise of the linescan needs to be improved.

322 Selection' function in the ImageJ interface, draw an ROI on an area of the STM that is in focus
323 and displays the most uniform and least intense area of fluorescence (F0).

I'm not sure what " an area of the STM that is in focus" means. If this is a confocal image there are no "out of focus" regions. The ROI should be placed on a uniform region with containing the lowest intensity.

The reviewer is correct, we have removed the emphasis on focus for this step of analysis.

362 that when the calibration bar is inserted, ImageJ creates a new STM containing it, leaving the
363 original version without the calibration bar intact and separate.

It didn't do this when I tried it.

If when inserting the calibration bar, the 'Overlay' box is ticked, then a new STM will not be created which may have happened to the reviewer in this instance. We have clarified this detail in the revised manuscript.

399 3.26 The velocity of a propagating Ca2+ event can be determined by drawing a line along the
400 propagating front of the event and calculating the slope of the line. This may be performed
401 manually in a similar manner described in step 3.24, by determining x,y values for where the
402 line begins (x1,y1) and ends (x2, y2), these values will be displayed in the lower left side of the
403 ImageJ interface when the mouse cursor is situated on the STM. Alternatively, plugins to
404 calculate velocity such as the 'Wave Speed' ImageJ plugin are available to download from
405 various sources.

This seems a rather time consuming process, it might be more useful to describe the use of the Wave Speed plug-in. Or alternatively write an ImageJ script to do it.

As stated above in response to reviewer 1, upon searching for the appropriate plugin online to provide a link, it appears that this plugin is now no longer available for public download and thus all reference to its use has been removed from the manuscript.

In a more general point here concerning this method Since once of the main arguments for the use of STMs was that they were more objective than simple fixed ROIs, I was slightly concerned to see that the identification of the Ca event by the placement of the horizontal and vertical is entirely manual.
I think something needs to be said here about how the user should go about selecting events consistently and objectively. Should every visible event be analysed for instance?

As per the reviewers suggestion we have included the following statement in our manuscript about consistently selecting Ca^{2+} signals for analysis. *"Note: Experimenters will need to design specific criterion for thresholding valid Ca^{2+} events in these recordings. In our experiments, we designated a Ca^{2+} event as being valid for analysis if its amplitude was >15% of the maximum amplitude event in the control section of recording. However, these thresholds will depend on the specific tissues and cells under study and are only arbitrary guidelines that require specific optimization for every type of tissue and cell."*

436 4.3 In order to accurately calculate Ca2+ signals from the entire FOV, the movie will firstly
437 undergo differentiation and smoothing to remove background interference and

increase the
438 signal to noise ratio. In the Movie Window, right click to bring up a menu and using right clicks
439 access 'STK Filter-Differentiate', right click again to input a value to differentiate, press ENTER

This needs further explanation. It's not clear what "differentiation" means in this context or why it should improve the signal-noise ratio? Also what sort of "background interference"?
I presume the smoothing is to increase the signal-noise ratio?

We have added the following statement to the manuscript to further clarify the differentiation function in Volumetry. "*Note: Differentiation in this context will reduce the intensity of areas of recording (pixels) that show no dynamic activity over the number of frames specified. Thus, if a value of '2' is inserted, each pixel in every frame of the recording is analysed and if within that frame there is no dynamic change in pixel fluorescence 1 frame before and 1 frame after, the intensity within those pixels will be subtracted from the recording. Thus non-dynamic background noise is removed and signal to noise is increased."*

The smoothing function does not affect signal to noise but helps in removing potential high frequency shot noise from the camera.

448 4.5 Start to create PTCLs by firstly selecting a quiescent period of the movie (20-40 frames)
.....
483 active Ca2+ transient PTCL at your determined threshold point. To save this as a coordinate

I find this whole section 448-483 hard to understand given the lack of explanation of what the aim of the processing is here. Since this is a very crucial part of the analysis it would benefit from being made clearer.
In the initial stage 4.5.-4.6, a threshold is determined semi-empirically from frames with no Ca activity isolating "particles" which correspond to the ICC-MY cells separated from background noise.
This threshold is then used throughout the analysis of subsequent frames? So is the intent to set the threshold just above the cell resting Ca fluorescence?
When Ca release events occur the number and area of a particles increase presumably because more of the ICC-MY cells area exceeds resting Ca conc.?

Can you define the criteria for selecting Ca release sites more explicitly and explain why it was chosen? E.g. why particles overlapping after 70 ms? Is this the expected duration of events?
I am also slightly puzzled about the criterion that there should be no overlap with another particle in the preceding frame.
If the threshold used to initially locate the cells during a quiescent period was used

to detect these particles then there would always be a particle present.
It would just get bigger in area when an event occurred. I may be misunderstanding something here.

Yes - the threshold equates to greater than the background intensity level of ICC-MY in the non-active state, i.e. during the inter slow-wave period. We have amended the text in the revised manuscript to make this more clear.

Indeed - events that transiently exceeded the "background" intensity level after both differentiation and smoothing filters were applied were considered as Ca^{2+} transients.

The choice to filter out Ca^{2+} events < 70ms was made mostly to filter out occasional random noise aggregations that could appear in 1 frame. These aggregations rarely lasted for more than 1 frame in the same spatial position and could be filtered temporally. The duration of Ca2+ transients was much longer (>150ms) and the temporal filter did not affect them.

Initiation particles had no overlap with other particles in the preceding frame - Ca2+ transient particles were overlapped through their duration.

The threshold choice, size + temporal filtering eliminated most/all background associated with labeled-cells in a transiently quiescent state. Therefore any particle was inherently a dynamic increase in Ca2+ intensity.

Minor Concerns:

203 2.4 Following this equilibration period, in situ Ca2+ imaging of small intestinal ICC-MY and
204 ICC-DMP can be performed using confocal microscopy. Due to the benefits of GECIs described
205 above, high-resolution time-lapse images (>30 frames per second, FPS) combined with high
206 power objectives (60-100x) can be used to acquire movies of dynamic Ca2+ signals in ICC.

Is it spinning disk confocal that is being referred to here, rather than point scanning. If so, better to be specific since a point scanning confocal would probably be operated in line scan mode obviating the need for the type of analysis described.

A spinning disc was in use here and we have specified this in our revised manuscript.

298 'Brightness/Contrast' (B&C). This will bring up a new heads up display (HUD) where various

299 aspects of brightness and contrast may be modified. Left click on the 'Auto' option once to
300 reveal the increased quality in the movie. Leave this B&C HUD open for future use.

Heads up display (HUD) is not a normal term for this. "pop-up dialog box", or just popup box would do.

We have amended our terminology from HUD to pop up box as the reviewer suggests.

Reviewer #4:
Manuscript Summary:
In situ calcium imaging provides an opportunity to study cellular activity within its native cellular environment. Cell-specific expression of genetically encoded calcium sensors has made it possible to perform high resolution Ca2+ imaging with low background and reduced photobleaching. However, there are a lack of techniques, particularly in enteric neuroscience for unbiased analysis of complex Ca2+ signaling patterns.
The authors outline a protocol to perform unbiased analysis of Ca2+ recordings from interstitial cells of Cajal (ICC) within the small intestine. They also quantify and describe the complex Ca2+ signaling patterns observed in ICCs located in different layers of the small intestine. The protocol describes two different approaches to quantify Ca2+ signals based on the pattern of cellular activity. They have used a spatiotemporal mapping based method (STM) for analysis of ICCs within the deep myenteric plexus, and a particle based technique for ICCs surrounding the myenteric plexus.
This protocol can be applied for extensive characterisation of complex subcellular Ca2+ signaling patterns in a cellular network. An advantage of the technique is the unbiased identification of regions within the field of view using a consistent thresholding protocol, as this can be a major source of operator error when defining ROIs. Using PTCL analysis, subcellular calcium signaling domains can be identified and characterized. The analytical techniques described can extract more quantitative data from Ca2+ recordings than traditional ROI-based methods, thus providing extensive spatial and temporal information.

Major Concerns:
NA

Minor Concerns:
*It is informative to see different analysis routines for varying cellular activity, but what about its applicability to other complex cell types or systems, such as enteric neurons and/or glia? Enteric glial cells also have slower calcium response profiles, in the order of seconds, depending on stimuli.

We have included a paragraph in the discussion describing how the PTCL based analysis outlined in this protocol has been applied to other complex tissues and suggest that it may also be applicable to neuronal networks also. *"PTCL analysis can be easily adapted to different intact preparations other than that described in this protocol. For example, a recent study used PTCL analysis to study novel rhythmic Ca^{2+} events occurring in the intact cellular networks of the lamina propria of the rat urinary bladder [55, 56] and thus could be easily applied to other complex, intact cellular systems such as neuronal systems."*

*It is a bit hard to follow the analysis routines in section 3 and 4. It will be helpful to include a flow chart giving an overview of the analytical steps.

We have simplified the analysis routines in section 3 and 4 and shortened the action steps. The protocol is now easier to follow and the design of figures 2-4 are provided in a step by step fashion to follow the text.

*It may be informative to give some background about the particle based analysis technique (advantages and principle?).

We have included a paragraph in our discussion outlining the advantages of using PTCL based analysis approaches to in situ imaging "*PTCL analysis provides a streamlined technique to quantify complex, subcellular Ca^{2+} events occurring in the network. Moreover, it also allows all Ca^{2+} events in the network within a given FOV to be analyzed, rather than using arbitrary ROIs, which only provide information on frequency and intensity within the ROI. An advantage of the PTCL analysis described here is that by applying differential and Gaussian smoothing filters to recordings, a large amount of noise can be removed from movies that may contain contaminating light from cells not of interest or due to non-dynamic bright spots or inclusions."*

*It appears that more information can be extracted from this data. What about analyzing the directionality and coordinated activity of the network?

This is certainly a possibility and in fact has been done for analyzing wave propagation directionality in a crude manner in ICC-MY (Drumm et al., 2017; J Gen Physiol). However, due to the length of the protocols already described we do not have enough space to include any detailed information on this possibility in the current manuscript.

*Authors should state the reason for using GCaMP6f, over GCaMP6 or GCaMP6s. It would be appropriate to mention this as the choice of GECI is dependent on the system being studied, and this in turn influences data analysis and interpretation.

We have included the following statement and reference in our revised manuscript to clarify our selection of GCaMP6f. *"Note: GCaMP6f was used due to its reported efficiency in reporting localized, brief intracellular Ca^{2+} signals in situ and in vivo. [54]"*

*Were any drugs added to reduce contractions (e.g. nicardipine)? If not, were there any movement artefacts (contractions/relaxations) during recording? Which motion stabilization algorithms or protocols were used (names)?

Nicardipine was applied during recordings to prevent tissue movement. The following statement has been inserted into the revised manuscript to clarify this. *"Note: To reduce tissue movement, nicardipine (0.1-1 μM) was applied during recordings as described previously.[37–41]"*

*In the long abstract, the authors should state that the technique focuses on analyzing data from GECIs.

We have included this point in the long abstract as suggested.

*This may fall outside the scope of the article, but the authors could add notes about using this same technique to analyze calcium dye loaded cells/tissue, i.e., whether the described technique can be used or not? If so, what are the considerations that must be taken into account? (Heppner et al., 2017)

We have added the following paragraph to the discussion of our revised manuscript to address this point "*While this paper focused on Ca^{2+} imaging in intact tissues with GECIs, these analysis techniques can also be run on isolated cells and tissues loaded with traditional Ca^{2+} indicator dyes. The STM based analysis has been used to successfully quantify localized Ca^{2+} signals and Ca^{2+} waves from spindle shaped interstitial cells and smooth muscle cells from a variety of preparations [11, 58–61]. Furthermore, the PTCL analysis routines described here have also been applied to in situ network preparations visualized with Cal 520 [56, 57]. However, these studies also retain the disadvantages of such dye loading protocols such as ambiguous cell identification and problems with signal to noise*."

Software:
*Will the steps for software analysis in the video be as detailed as the protocol, i.e., will the video include step by step instructions for software use?

Certain steps will be included in the video as decided by the JOVE editorial team.

*Including an ImageJ macro for steps outlined in section 3 will ensure accurate reproducibility of the protocol. It could also be a list of the commands from the ImageJ 'Macro Recorder window'.

As the selection of regions for background noise, F_0 and lines to be drawn for linescans require drawing lines and ROIs on different regions of the movies / cell and these are different in every recording, we do not feel that a Macro for the detailed analysis described in section 3 would be beneficial for users at this time.

*Can ImageJ be used for section 4?

Image J does have the capability for pixel based PTCL analysis routines. However, the design and implementation of such routines is not conducted in our laboratory and all PTCL based analysis is conducted using the Volumetry software as described.

*Please include a link or reference to the 'Wave Speed' ImageJ plugin (section 3.26).

As stated above in response to reviewer 1, upon searching for the appropriate plugin online to provide a link, it appears that this plugin is now longer available for public download and thus all reference to its implication has been removed from the manuscript.